NAC-0032_R3

Deep Time Assessment for the Clive DU PA

Clive DU PA Model v1.2

5 August 2014

Prepared by

NEPTUNE AND COMPANY, INC.

1505 15th St, Suite B, Los Alamos, NM 87544

1. Title: Deep Time Assessment for the Clive DU PA		
2. Filename: Deep Time Assessment v1.2.docx		
3. Description: This report describes details of the "deep time" component of the Clive DU PA Model. The "deep time" model addresses long term effects (beyond 10,000 years post-closure) of disposal of DU at the Clive facility.		
	Name	Date
4. Originator	Michael Balshi	31 May 2014
5. Reviewer	Mike Sully, Paul Black	31 May 2014
6. Remarks 3 Jul 2014; R2: Accepted track changes from R1 and added "a" and "b" to identify two Oviatt et al. (1994) references – D. Levitt 30 Jul 2014: Updates and corrections for v1.2. White Paper now at rev 3. — R. Lee and J. Tauxe 31 Jul 2014: Additional editorial changes. Accepted all tracked changes. Comments need to be addressed. Changed authorship to M. Balshi, as the original work was done by him. –R. Lee		

This page is intentionally blank, aside from this statement.

CONTENTS

FIGURES

TABLES

1.0 Deep Time Scenarios Distribution Summary

The following is a brief summary of input values used parameters employed in the deep time[1] scenarios component of the Clive Performance Assessment (PA) model that is the subject of this white paper.

For distributions, the following notation is used:

- LN(*GM*, *GSD*, [*min*, *max*]) represents a log-normal distribution with geometric mean GM and geometric standard deviation GSD, and optional *min* and *max* if truncation is needed, and
- Beta(μ, σ, *min*, *max*) represents a generalized beta distribution with mean μ, standard deviation σ, minimum *min*, and maximum *max*.

Table 1. Summary of distributions for the Deep Time Scenarios container

Model Parameter	Value or Distribution	Units	Reference
start time for deep lake	LN(GM = 14000, GSD = 1.2, min = 0, max = 50,000)	yr	Section 6.1
end time for deep lake	LN(GM=6000, GSD=1.2, min=0, max=50,000)	yr	Section 6.1
deep lake sedimentation rate	LN(GM = 0.00012, GSD = 1.2)	m/yr	Section 6.3
duration of intermediate lake	LN(GM = 500, GSD = 1.5, min = 0, max = 2,500)	yr	Section 6.2
sediment thickness for intermediate lake	LN(GM = 2.82, GSD = 1.71)	m	Section 6.3
site dispersal area	LN(GM = VolumeAboveGrade / 0.1 m, GSD = 1.5, min = VolumeAboveGrade / 1 m, max = Large*)	km^2	Section 6.4
depth of intermediate lake	beta(μ = 30, σ = 18, min = 0, max = 100)	m	Section 6.5
depth of deep lake	beta(μ = 150, σ = 20, min = 100, max = 200)	m	Section 6.5

* "Large" is a very large number defined in the Clive DU PA Model.

[1]For the purpose of this white paper, deep time refers to the period between 10 thousand years to 2.1 million years

2.0 Deep Time Scenarios Overview

There are two major components to the Clive depleted uranium (DU) Performance Assessment (PA) Model. The first addresses quantitative contaminant fate and transport and subsequent dose assessment for 10,000 years (10 ky) and is based on projections of current societal conditions into the future, and assumes no substantial change in climatic conditions. The second addresses deep time scenario calculations until the time of peak radioactivity. For this PA, peak radioactivity associated with the ingrowth of progeny from ^{238}U occurs at about 2.1 million years in the future (My).

The basic deep time scenario involves projecting the future environment based on the past. The conceptual model of the past environment is based on scientific records (sediment borehole logs, ice cores, deep ocean cores) of the past eight glacial/climate cycles that have lasted approximately 100 ky each. We are currently in an interglacial period. The model considers cycles from the near beginning of an interglacial period onwards. In the past 100-ky cycles, after the interglacial period, the average temperature drops and average precipitation increases throughout the cycle, until the relatively cold period (typically an 'ice age') ends, and the next interglacial period begins.

The deep time component requires consideration of climatic changes that have occurred on approximately 100-ky cycles for more than 1 My, based on scientific literature. These cycles include periods of extensive glaciation and interglacial periods, as illustrated in Figure 1. Earth is currently in an interglacial period. In effect, the first 10 ky of the Clive DU PA Model is projected under interglacial conditions, and the deep time calculations include an evaluation of the effect on DU disposal in the Federal DU cell of future 100-ky glacial cycles for the next 2.1 My.

The objective of the deep time calculations in the Clive DU PA Model is to assess the potential impact of glacial epoch pluvial lake events on the overall DU waste embankment from 10 ky through 2.1 My post-closure. A pluvial lake is a consequence of periods of extensive glaciation, and results from low evaporation, increased cloud cover, increased albedo, and increased precipitation in landlocked areas.

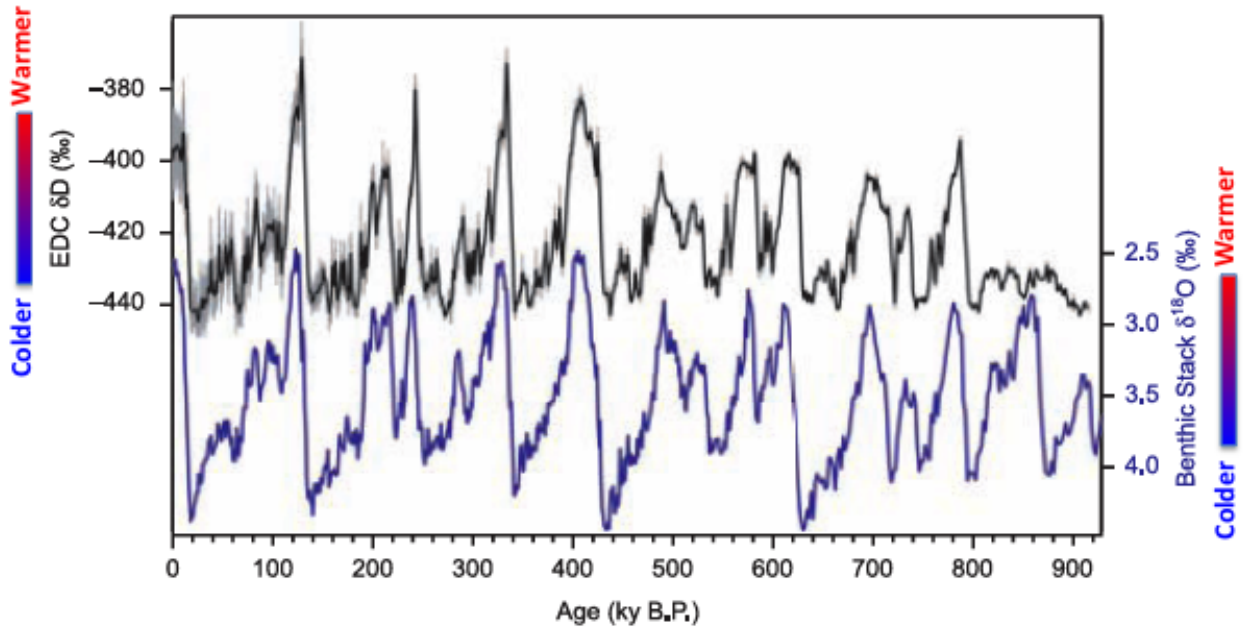

Figure 1. Comparison of delta deuterium (black line) from the European Project for Ice Coring in Antarctica (EPICA) Dome C ice core and benthic (marine) oxygen-18 record (blue line) for the past 900 ky [from Jouzel et al. (2007)]

The deep time evaluation focuses on potential releases of radioactivity following a series of lake events caused by glacial cycles (Figure 1). The approximate 100-ky glacial cycles can be easily discerned in Figure 1. The current interglacial period is shown on the left edge of the figure. The last ice age finished between 12,000 and 20,000 years ago (12 ka and 20 ka, annotated as "ky B.P." in the figure). Around the last glacial maximum (represented as a trough on the far-left side of Figure 1), Lake Bonneville reached its maximum extent. The ice core data and the benthic marine isotope data show very similar patterns for the past 800 ky. These 100-ky cycles are used as the basis for modeling the return and recurrence of lake events in the Bonneville Basin.

The approach to deep time modeling is also briefly described in the *Conceptual Site Model for Disposal of Depleted Uranium at the Clive Facility* (Neptune, 2014a). The model is developed further here, including more detailed conceptual model development, model structuring and model specification based on available data, scientific literature, and expert opinion.

For the deep time evaluation, the Clive DU PA Model provides an assessment of plausible future environmental consequences of present-day disposal of DU waste. Doses to potential human receptors are *not* calculated. However, projected concentrations of radioactive species are tracked in both lake water and lake sediments. Although the 100-ky glacial patterns can be used as a basis for modeling lake recurrence, specific temporal information available for assessing the long-term behavior of the DU waste disposal system and the area surrounding the Clive site is highly uncertain. Although large, deep lakes are expected to return, the exact timing is uncertain. However, the exact timing is not important. What is important is that the Model allows for

periodic recurrence of deep lakes, similar to those that have occurred in the past, that could inundate the Clive area in the future. With this approach, the impact of deep lakes on the disposal system can be evaluated in the spirit of the Utah regulations (qualitative assessment with simulations).

The deep time scenario should be regarded as conceptual and stylized. The intent is to present a picture of what the future might hold for the Federal DU Cell, rather than to provide a quantitative, temporally specific, prediction of future conditions, or an assessment of exposure or dose to human receptors who might or might not exist long into the future. Given the large uncertainties involved in predicting the long-term future, a more detailed model would be exceedingly speculative. The type of glacial climate change envisioned in the deep time scenario will probably have wide-reaching consequences for the planet, far beyond the scope of a PA.

The focus of the deep time evaluation is the return of deep lakes in the Bonneville Basin.. Other less likely geologic events could also occur in the next 2.1 My. Events such as meteorite impacts, and volcanic activity such as in the Yellowstone Caldera could also be considered. Future volcanic events are often screened from consideration in PAs on the basis of a low probability of occurrence and/or limited consequences. In this case, a major meteorite impact and a future volcanic eruption at Yellowstone were not screened. Instead, the impacts of these events are considered to be so catastrophic on a global scale that their effects on low-level radioactive waste disposal at Clive are literally inconsequential.

Lava dams in the northern parts of the historic Lakes Thatcher and Bonneville affected the transgressive (rise) and regressive (drainage) history of the lakes during the Pleistocene (Link et al., 1999), and volcanic activity likely affected drainage into Lake Bonneville during and following the last glacial maximum. Basaltic volcanic eruptions associated with the Black Rock Desert volcanic field (Nash, 1990) pre-date, were contemporaneous with, and post-date the multiple stages of Lake Bonneville (Nash, 1990; Oviatt and Nash, 2014). Volcanic eruptions near the Clive site are low probability events in the next 10 ky. However, Quaternary basaltic and rhyolitic eruptions occurred along the length of the eastern margin of the Great Basin (north-south zone through central Utah) and will likely occur again within the Bonneville lake region during the 2.1-My interval of the deep time scenario. These future events will likely affect anticipated glacial lake cycles.

The background sections provide a detailed overview of past climatic conditions that have been linked to the formation of pluvial lake events in the Bonneville Basin, which is the large drainage basin in Utah that has been subject to pluvial lake events in the past. For example, the Great Salt Lake is a remnant of Lake Bonneville, the pluvial lake that existed at the last glacial maximum. These background sections are followed by a presentation of the conceptual site model and the specific functions and parameters implemented in the deep time scenarios in the Clive DU PA Model.

3.0 Background on Pluvial Lake Formation in the Bonneville Basin

3.1 Long-term Climate

Large-scale climatic fluctuations over the last 2.6 My (the beginning of the Quaternary Period in geologic time) have been studied extensively in order to understand the mechanisms underlying those changes (Hays et al., 1976, Berger, 1988, Paillard, 2001, Berger and Loutre, 2002). These climatic signals have been observed in marine sediments (Lisiekcki and Raymo, 2005), land records (Oviatt et al., 1999), and ice cores (Jouzel et al., 2007). These large-scale fluctuations in climate have resulted in glacial and interglacial cycles, which have waxed and waned throughout the Quaternary Period. The causes of the onset of the last major northern hemisphere glacial cycles 2.6million years ago (Ma) remain uncertain, but several studies suggest that the closing of the Isthmus of Panama caused a markèd reorganization of ocean circulation patterns that resulted in continental glaciation (Haug and Tiedemann, 1998, Driscoll and Haug, 1998). Future glacial events are likely to be caused by a combination of the Earth's orbital parameters as well as increases in freshwater inputs to the world's oceans resulting in a disruption to oceanic thermohaline circulation (Driscoll and Haug, 1998).

Changes in the periodicity of glacial cycles have been linked to variations in Earth's orbit around the Sun. These variations were described by Milankovitch and are based on changes that occur due to the eccentricity (i.e., orbital shape) of Earth's orbit every 100 ky, the obliquity (i.e., axial tilt) of Earth's axis every 41 ky, and the precession of the equinoxes (or solstices) (i.e., wobbling of the Earth on its axis) every 21 ky (Berger, 1988). For the first 2 My of the Pleistocene (the first major Epoch of the Quaternary Period), Northern Hemispheric glacial cycles occurred every 41 ky, while the last million years have indicated glacial cycles occurring every 100 ky, with strong cyclicity in solar radiation every 23 ky (Berger and Loutre, 2002; Paillard, 2006). The shift from shorter to longer cycles is one of the greatest uncertainties associated with utilizing the Milankovitch orbital theory alone to explain the onset of glacial cycles (Paillard, 2006).

The evaluation by Hays et al. (1976), who analyzed changes in the isotopic oxygen-18 ($\delta^{18}O$) composition of deep-sea sediment cores, suggest that major climatic changes have followed both the variations in obliquity and precession through their impact on planetary insolation (i.e., the measure of solar radiation energy received on a given surface area in a given time). In its most common form, oxygen is composed of eight protons and eight neutrons (giving it an atomic weight of 16). This is known as a "light" oxygen because a small fraction of oxygen atoms have two extra neutrons and a resulting atomic weight of 18 (^{18}O), which is then known as "heavy" oxygen. ^{18}O is a rare form and is found in only about 1 in 500 atoms of oxygen. The ratio of these two oxygen isotopes has changed over the ages and these changes are a proxy to changing climate that have been used in both ice cores from glaciers and ice caps, and cores of deep sea sediments. Thus, variations in $\delta^{18}O$ reflect changes in oceanic isotopic composition caused by the waxing and waning of Northern Hemispheric ice sheets, and are thus used as a proxy for previous changes in climate (*cf*. Figure 1).

Slightly different external forcing and internal feedback mechanisms can lead to a wide range of responses in terms of the causes of glacial-interglacial cycles. The collection of longer ice core records, such as the European Project for Ice Coring in Antarctica (EPICA) Dome C core located

in Antarctica, has highlighted the clear distinctions between different interglacial-glacial cycles (Jouzel et al., 2007). Variation in climatic conditions appears to be sufficient that large differences have occurred in each of the past several 100-ky cycles. At the present time, the EPICA Dome C core is the longest (in duration) Antarctic ice core record available, covering the last 800 ky (Jouzel et al., 2007).

Note that there is considerable uncertainty associated with the number, timing, and recurrence interval of lakes in the Bonneville Basin. The 100-ky glacial cycle is roughly correlated with the occurrence of deep lakes (Balch et al. 2005, Davis 1998), and there appear to be smaller, millennial scale ("Dansgaard-Oeschger") cycles within this larger cycle that are not necessarily uniform (Madsen, 2000). For example, the Little Valley lake cycle peaked in elevation at about 135 ka, the Cutler Dam lake cycle peaked about 65 ka, and the Bonneville lake cycle peaked about 18 ka (Machette et al., 1992). The following sections discuss these cycles in more detail.

Many studies highlight the importance of past atmospheric composition in the dynamics of glaciations across the Northern Hemisphere, in addition to the insolation due to orbital influences (Masson-Delmotte et al., 2010; Clark et al., 2009; Paillard, 2006). Carbon dioxide (CO_2) is a well-known influence on the atmospheric "greenhouse effect" (i.e. warming due to trapping of solar heat), and is a globally well-mixed gas in the atmosphere due to its long lifetime. Therefore, measurements of this gas in Antarctic ice are globally representative and provide long-term data important for understanding past climatic changes. Direct measurement of CO_2 trapped in the EPICA Dome C core indicates that atmospheric CO_2 concentrations decreased during glacial periods due to greater storage in the deep ocean, thereby causing cooler temperatures from a reduction of the atmosphere's greenhouse effect (EPICA, 2004). Warmer temperatures resulting from elevated concentrations of CO_2 released from the ocean contribute to further warming and could support hypotheses of rapid wasting at the end of glacial events (Hays et al., 1976). Earlier interglacial events (prior to 420 ka), however, are thought to have been cooler than the most recent interglacial events (since 420 ka) (Masson-Delmotte et al., 2010).

Berger and Loutre (2002) conducted simulations including orbital forcing coupled with insolation and CO_2 variations over the next 100 ky. Their results indicated that the current interglacial period could last another 50 ky with the next glacial maximum occurring about 100 ky from now. The scientific record (*cf*. Figure 1) supports variability across the 100-ky glacial cycles. Berger and Loutre (2002) effectively indicate that the current 100-ky cycle will not be as glacially intense as some of the previous cycles. They also quote J. Murray Mitchell (Kukla et al, 1972, p. 436) who predicts that "The net impact of human activities on climate of the future decades and centuries is quite likely to be one of warming and therefore favorable to the perpetuation of the present interglacial." Archer and Ganopolski (2005) conducted simulations suggesting that the combination of relatively weak orbital forcing and the long atmospheric lifetime of carbon release from fossil fuel and methane hydrate deposits could prevent glaciation for the next 500 ky over two glacial cycle eccentricity minima. Cochelin et al. (2006) used a paleoclimate model with interactive vegetation to simulate the next glacial inception under orbital and atmospheric CO_2 forcings. The model produced three states: an impending glacial inception under low CO_2 levels, a glacial inception in 50 ky for CO_2 levels of 280 to 290 ppm, or no glacial inception for the next 100 ky for CO_2 levels of 300 ppm or higher. Tzedakis et al. (2012a) defined interglacial periods as episodes where global climate is incompatible with the wide global extent of glaciers, and examined differences in interglacial

durations over the last 800 ky. They noted that the onset of interglacials occurs within 2 ky of the boreal summer insolation maximum consistent with Milankovitch forcing whereas the end of interglacials does not occur consistently on a similar part of the insolation curve. Reduction in summer insolation is identified as a primary trigger for glacial inception but multiple other feedbacks including atmospheric CO_2 concentrations combine to amplify the timing of glacial inception. They further recognized two main groups for mean duration of interglacials: 13±3 ky and 28±2 ky. In a related paper, Tzedakis et al. (2012b) suggest that the end of the current interglacial could occur within the next 1,500 years if atmospheric CO_2 concentrations do not exceed about 240 ppm, but no glacial inception is projected to occur at current atmospheric CO_2 concentrations of 400 ppm, consistent with the conclusions of Archer and Granopolski (2005). Jansen et al. (2007) in Chapter 6 of the fourth assessment report of the Intergovernmental Panel on Climate Change (IPCC) concluded that "It is very unlikely that the Earth would naturally enter another ice age for at least 30 ky." These conclusions were updated and strengthened in Chapter 5 of the fifth IPCC assessment report (Masson-Delmotte et al., 2013).

Predicting future climate states including the potential impact of anthropogenic CO_2 (as opposed to natural sources) is both controversial and uncertain. Although anthropogenic influences are likely to extend the current interglacial period, this potential effect is not considered in the deep time scenario. Orbital forcing is assumed to dominate glacial cycles for the duration of the modeling study (2.1 My). This approach could be updated, if considered important, based on further consideration of the effect of anthropogenic CO_2 forcing upon future glaciation in a revised PA model

Berger and Loutre (2002) report that future increases in atmospheric CO_2 from anthropogenic activity along with small insolation variations could result in a transition between the Quaternary and the next geologic period due to the potential wasting of the Greenland and West Antarctic Ice Sheets. However, such melting would also result in increased freshwater inputs to the oceans and could cause a shift toward a colder climate and the next glacial age (Driscoll and Haug, 1998).

Other gases, such as deuterium (^2H), have also been measured in the EPICA Dome C core. Jouzel et al. (2007) assembled a high-resolution deuterium profile from the EPICA Dome C core and used these measurements to extend the climate record back to 800 ka (see Figure 1). These data indicate that a 100-ky periodicity primarily dominates the temperature record, but the record also indicates that a strong obliquity (40- to 41-ky) component exists and increases when going from past to present. Jouzel et al. (2007) also indicate that in general, systematic millennial-scale changes are related to North Atlantic deep water formation (influenced by fresh water inputs and sea ice formation), which is shown for the last glacial cycle and suggested for previous glacial periods.

Given the uncertainties involved in these studies, the deep time model focuses on stylized projection of the past 800 ky of 100-ky glacial cycles, without consideration of anthropogenic CO_2 effects.

The following sub-sections present an overall background on past events in the Bonneville Basin that are driven by major shifts in climatic regime that are presumed to occur in the future (10 ky to 2.1 My).

3.2 Deep Lake Cycles

The Bonneville Basin is the largest drainage basin in the Great Basin of the Western United States. It is a hydrologically closed basin of over 134,000 km^2, and has previously been occupied by deep pluvial lakes. Pluvial lakes typically form when warm air from arid regions meets chilled air from glaciers, creating cloudy, cool, rainy weather beyond the terminus of the glacier. The increase in rainfall and moisture can fill the drainage basin, forming a lake. This kind of humid climate was evident during the last glacial period in North America, and resulted in more precipitation than evaporation, hence the rise of Lake Bonneville.

Numerous studies have investigated previous lake cycles in the Bonneville Basin. These include studies of Lake Bonneville shoreline geomorphology (Currey et al., 1984), palynological (i.e., pollen) studies of deep boreholes (Davis, 1998), and studies of the geochemistry of deep-water lacustrine depositional sequences (Eardley et al., 1973; Oviatt et al., 1999, Balch et al., 2005). Analysis of these sediment cores is used to help understand previous lake levels and characteristics as well as establish the approximate age of previous lake cycles (e.g., Oviatt et al., 1999).

Oviatt et al. (1999) analyzed hydrolysate amino acid enantiomers for aspartic acid, which is abundant in ostracode protein. Ostracodes are small crustaceans that are useful indicators of paleo-environments because of their widespread occurrence and because they are easily preserved. Ostracodes are highly sensitive to water salinity and other limnologic changes. Therefore, portions of sediment cores that contain ostracodes indicate fresher, and hence probably deeper, lake conditions than the modern Great Salt Lake (Oviatt et al., 1999). To establish the approximate timing of previous lake cycles, Oviatt et al. (1999) examined sediments from the Burmester sediment core originally collected in the early 1970s near Burmester, Utah (Eardley et al., 1973). Burmester is approximately 65 km east of Clive on the southern edge of the Great Salt Lake, at an elevation of 1286 m above mean sea level (amsl). The Clive are has an elevation of 1307 m amsl. Oviatt has also collected sediment data from Knolls (to the west of Clive) and at Clive itself (described further in Section 3.3). These data are largely consistent with the more recent layers from Burmester, indicating similar sedimentation processes at work at least during these time periods.

Data from the 307-m Burmester core suggest that a total of four deep-lake cycles occurred during the past 780 ky (Table 2). Oviatt et al. (1999) found that the four lake cycles correlated with marine $\delta^{18}O$ stages 2 (Bonneville lake cycle: ~24 to 12 ky), 6 (Little Valley lake cycle: ~186 to 128 ky), 12 (Pokes Point lake cycle: ~478 to 423 ky), and 16 (Lava Creek lake cycle: ~659 to 620 ky).

Oxygen isotope stages are alternating warm and cool periods in the Earth's paleoclimate which are deduced from oxygen isotope data (Figure 2). These correlations suggest that large pluvial lake formation in the Bonneville Basin occurred in the past only during the most extensive Northern Hemisphere glaciations. There are many interacting mechanisms that could control or 'force' glaciation and deglaciation. For example, Oviatt (1997) and Asmerom et al. (2010) suggested that these extensive glaciations were controlled by the mean position of storm tracks throughout the Pleistocene, which were in turn controlled by the size and shape of the ice sheets. Other glaciation forcing mechanisms have been suggested. The review by Ruddiman (2006) suggests that insolation changes due to orbital tilt and precession, greenhouse gas concentrations,

changes in Pacific Ocean circulation, and possibly other interacting mechanisms could contribute to glaciation and deglaciation cycles in North America, and thus pluvial lake existence and size. Lyle et al. (2010) suggests that lake levels in the Pleistocene western US were influenced by stronger spring/summer precipitation fed by tropical Pacific air masses, rather than higher numbers of westerly winter storms. Regardless, the high-level, conceptual modeling of lake cycles that was conducted here did not assume any particular mechanism of glaciation and deglaciation. For example, the modeling simply assumed a 100-ky cycle, regardless of the mechanism.

Balch et al (2005) conducted a more recent detailed study on ostracode fossils in Great Salt Lake sediment (i.e., under the lake). Other fossil invertebrates were also used as paleoecological indicators in this study. Both brine shrimp and brine fly fossils are indicators of hypersaline environments because they have a much higher salinity tolerance than most other invertebrates. This study's findings were consistent with Oviatt et al.'s (1999) later cycles, but as the core was not as deep the findings are not as useful for the present purpose as the Burmester data. The Burmester core data are more germane to the present modeling effort because they represent a relatively long time period in which to establish the occurrence of pluvial lakes in the region. However, note that there is considerable uncertainty associated with the number, timing, and recurrence interval of lakes in the Bonneville Basin. The 100-ky glacial cycle is roughly correlated with the occurrence of deep lakes (Balch et al., 2005; Davis, 1998), and there appear to be smaller, millennial-scale cycles within this larger cycle that are not necessarily uniform (Machette et al., 1992; Madsen, 2000). It is likely that shallow lakes have also occurred in each glacial period, but the shorelines have been destroyed by later lakes. Sediment mixing that occurs during lake formation can also mask the existence of previous shallow lakes. Thus, it is impossible to have complete confidence in historical lake formation characteristics and formation.

Regardless, deep lakes have occurred in the past, as have intermediate lakes and shallow lakes. The model addresses this history by allowing deep lakes to return in some glacial cycles, and by allowing intermediate lakes to occur as part of the transgressive and regressive phases of lake development.

Table 2. Lake cycles in the Bonneville Basin during the last 700 ky[1]

Lake Cycle	Approximate Age[2]	Maximum Elevation	Lake level control
Great Salt Lake (current level)	present	1284 m (4212 ft) in 1873	Interglacial climate; human intervention
Bonneville (Gilbert Shoreline)	12.9 to 11.2 ka	1295 m (4250 ft)	Beginning of interglacial climate; possible regressive phase of Lake Bonneville; possible association with the Younger Dryas period
Bonneville (Provo Shoreline)	17.4 to 15.0 ka	1445 m (4740 ft)	Glacial climate; new threshold at Zenda near Red Rock Pass, Idaho (natural dam collapse)
Bonneville (Bonneville Shoreline)	18.3 to 17.4 ka	1552 m (5090 ft)	Glacial climate; threshold at Zenda near Red Rock Pass, Idaho
Bonneville Transgression	~30 to 18.3 ka		Glacial climate
Bonneville (Stansbury Shoreline)	26 to 24 ka	1372 m (4500 ft)	Glacial climate; transgressive phase of Lake Bonneville
Cutler Dam	~80 to 40 ka	<1380 m (<4525 ft)	Glacial climate
Little Valley	~128 to 186 ka	1490 m (4887 ft)	Glacial climate
Pokes Point	417 to 478 ka	1428 m (4684 ft)	Glacial climate
Lava Creek	~620 to 659 ka	1420 m (4658 ft)	Glacial climate

Elevations are not corrected for isostatic variations.
[1] Note the various levels of the last major lake cycle, Lake Bonneville.
[2] Approximate ages derived from Currey, et al. (1984) Link et al. (1999) and Oviatt et al. (1999). Bonneville cycle approximate age presented as calibrated years.

Lake Bonneville is the last major deep lake cycle that took place in the Bonneville Basin and is widely described in the literature (Hart et al., 2004; Oviatt and Nash, 1989; Oviatt et al., 1994a, 1999). Lake Bonneville was a pluvial lake that began forming approximately 28 to 30 ka, forming various shorelines throughout its existence and covering over 51,000 km^2 at its highest level (Matsurba and Howard, 2009).

Most studies indicate that the high-stand (i.e., the highest level reached) of the lake at the Zenda threshold (1,552 m amsl), located north of Red Rock Pass, occurred approximately 18.3 to 17.4 ka. The high-stand of the lake was followed by an abrupt drop in lake level due to the catastrophic failure of a natural dam composed of unconsolidated material at approximately 17.4 ka. As a result of this flood, the lake dropped to a level of 1,445 m amsl, called the Provo level. The Provo level is the maximum level that any future deep lake is likely to reach without major regional tectonic changes (Currey et al., 1984; Oviatt et al., 1999). A more recent study (Miller et al., 2013), using radiocarbon dating for Provo shoreline gastropod deposits, estimates

that the dam collapse and Bonneville flood event occurred between 18.0 and 18.5ka, and therefore the high-stand may have occurred earlier. However, Miller et al. (2013) indicate that "uncertainties in [gastropod] shell ages may be as large as thousands of years, and the major shorelines of Lake Bonneville and the Bonneville flood require more work to establish a reliable chronology." The lake regressed rapidly during the last deglaciation, then increased again to form the Gilbert shoreline between 11.2 to 12.9 ka, which coincided with the Younger Dryas global cooling event (Oviatt et al., 2005).

The lake then receded to levels of the current Great Salt Lake at approximately 10 ka for the remainder of the Holocene Epoch.

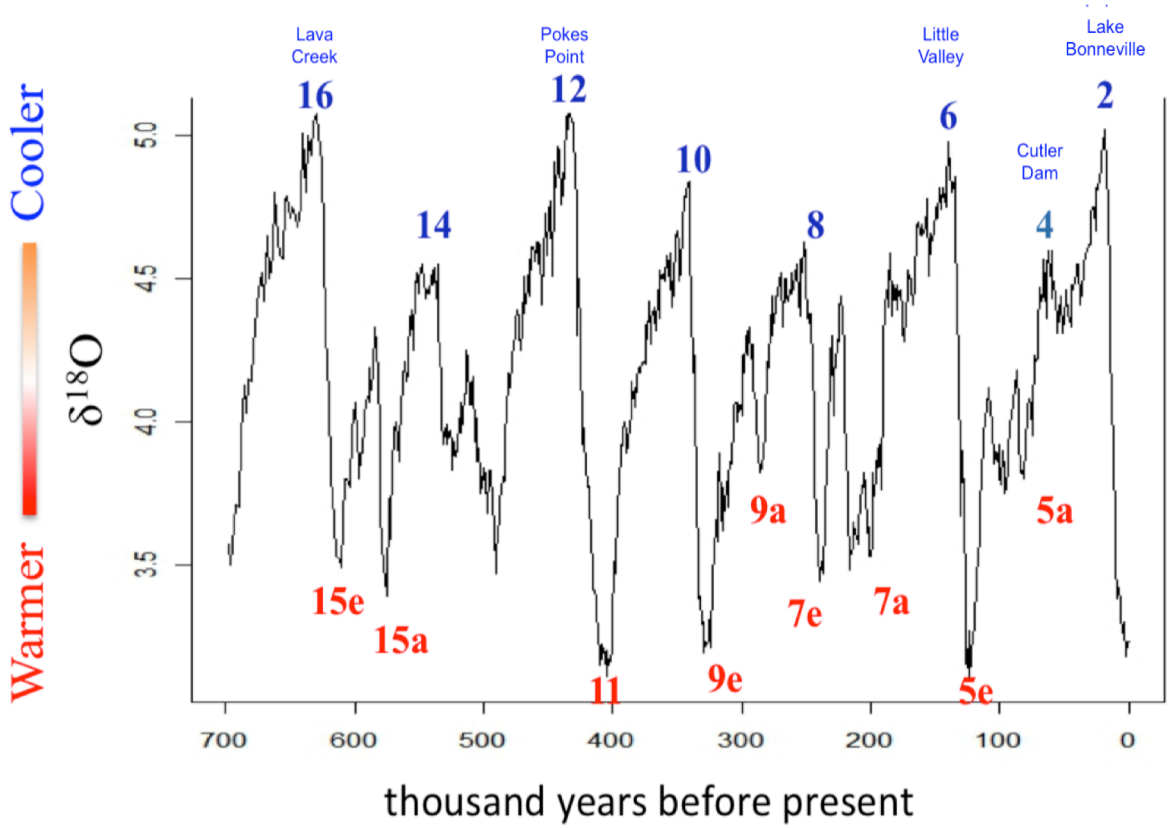

Figure 2. Benthic oxygen isotope record for the last 700,000 years (from Lisiecki and Raymo, 2005)[2]

Glacial cycles can be discerned in Figure 2 by considering each cycle from the beginning of the interglacial period and ending each cycle at the peaks that correspond to deep lake occurrence. Using this approach, the current glacial cycle started around 12 ka, Lake Bonneville occurred at the end of the last complete cycle, and Cutler Dam occurred in the middle of the last 100-ky

[2]Red (warm periods) and blue (cool periods) values correspond to marine isotope stages based on Lisiecki and Raymo (2005). Lake stages identified by Oviatt et al. (1999) are also included in blue text.

cycle. The previous 100-ky cycle resulted in Little Valley. Pokes Point occurred five cycles ago, and Lava Creek seven cycles ago. These deep lakes have been identified in sediment cores and in shorelines around the Bonneville Basin. However, it is likely that many more shallow lakes have also occurred in each glacial period, but the shorelines have been destroyed by subsequent deeper lakes.

Sedimentation in the Bonneville Basin is caused by several factors including air dispersion in interglacial periods, and both terrigenous and biogenic sedimentation when lakes are formed in glacial periods. Sedimentation also depends on location within the basin, which governs river input, wave energy, sediment availability on piedmonts, water chemistry, biological activity, and slope. The mixing of sediment that occurs during lake formation can mask the existence of previous relatively shallow lakes. There is considerable uncertainty in the number of lakes of various sizes that might have existed in the Bonneville Basin. However, the main focus of the deep time scenario modeling is to evaluate the presence of lakes that inundate Clive at different times in future glacial cycles, and to approximately match the net sedimentation of the past glacial cycles.

3.3 Shallow and Intermediate Lake Cycles

For modeling purposes, a distinction is made between shallow, intermediate and deep lakes.

- Deep lakes are assumed to be similar to Lake Bonneville or Lake Provo, and occur no more than once per 100-ky glacial cycle (assumption of the heuristic model approach).
- Intermediate lakes are assumed to be smaller lakes that reach and exceed the altitude of Clive, but are not large (or deep) enough that carbonate sedimentation is the dominant mode of lake deposition. The Bonneville and Provo shorelines are examples of deep lakes.The transgressive and regressive phases of the Bonneville and Provo shoreline lakes represent intermediate lakes during the transient phases where they exceeded the elevation of Clive and sedimentation was dominated by clastic deposition associated with wave activity and reworking of lake sediments (see Table 2 for the chronology of the lake cycles).
- Shallow lakes are assumed to exist at all other times, but these are irrelevant to the geomorphology of the Clive site.

The current Great Salt Lake is an example of a shallow lake, as is the reinterpreted Gilbert shoreline lake (Oviatt, 2014) that has now been shown to not have reached the elevation of the Clive site (contrast with Currey et al., 1984). The specific depths of shallow, intermediate and deep lakes are not important in the Deep Time Model. Under current climate conditions, -only shallow lakes will occur. Under future climate conditions, some glacial cycles will produce deep lakes in the Bonneville Basin, and intermediate lakes will occur during the transgressive and regressive phases of deep lakes, or during glacial cycles that do not produce deep lakes. The approximate timing of the return of the first intermediate lake is relatively important in the Deep Time Model, because it is assumed that the Clive waste disposal site is destroyed upon the occurrence of the first intermediate lake.

A key assumption for the deep time assessment is the observation, based on core sediment studies, that the net depositional rate of deep lakes is lower than the sediment depositional rate for intermediate lakes. The conceptual basis for this assumption is that sedimentation rates are

dependent on basin location, presence or absence of fluvial deposition, wave dynamics, availability of local sediment sources, slope, water chemistry and biological activity. Biogenic carbonate deposition is likely to occur under a wide range of lake conditions, but the ratio of carbonate deposition to clastic sedimentation will increase as the lake deepens because of the reduction in sedimentary influx with increased distance from shoreline processes and decreased wave activity.

There are recognized trends in carbonate mineralogy that can be correlated with lake volume and indirectly lake depth (for example, Oviatt, 2002; Oviatt et al., 1994b; Benson et al., 2011). The transitions from low-magnesium calcite to high-magnesium calcite to aragonite generally reflect increasing lake salinity and increasing magnesium concentration, which occur with decreasing lake volume. Similarly, for a hydrologically closed pluvial lake system, the relative concentration of total inorganic carbon should decrease as lake size increases. The $\delta^{18}O$ of deposited carbonate can be correlated with rising lake levels because of the interplay between the $\delta^{18}O$ value of river discharge entering a lake and the $\delta^{18}O$ value of water vapor exiting the system via evaporation (Benson et al., 2011). The mineralogy and isotopic composition of carbonate composition can be obtained from sediment cores. However, interpretation of the data is complicated by multiple processes, including: local groundwater discharge, introduction of glacial rock flour, and reworking of lake sediments during transgressive and regressive lake cycles.

The model parameters used in the deep time assessment are sensitive to lake duration and sedimentation rates but are not dependent on the dynamics of carbonate deposition. Radionuclides in sediment will partition between the lake water and solid phase dependent on element-specific solubility and assigned sorption properties. Radionuclides remaining in the pore water can diffuse into the lake water. Some radionuclide species may bind with carbonate ions in the lake water and precipitate as carbonate. However, the deep time assessment conservatively assumes all waste is precipitated with and incorporated into local sediments during lake recession.

Intermediate lake events have occurred in the Clive area. These are documented in Table 3 (C.G. Oviatt, Professor of Geology, Kansas State University, personal communication December 2010, January 2011, and email communication herein referred to as "C.G. Oviatt, personal communication". This information was updated in April 2014; see the caption for Table 3). These events are evident from a pit wall interpretation at the Clive site (Appendix A; C.G. Oviatt, unpublished data) as well as at the ostracode and snail record present in the Knolls sediment core (12 km west of Clive near the Bonneville Salt Flats; Appendix B; C.G. Oviatt, unpublished data). The pit wall study conducted by Oviatt occurred during early development of the Clive disposal facility. From the Clive pit wall interpretation, it is presumed that at least three intermediate lake cycles occurred prior to the Bonneville cycle, although there is uncertainty associated with that estimate. For example, these intermediate cycles could in fact be part of the transgressive phase (i.e., rising lake level) of the Lake Bonneville cycle (C.G. Oviatt, personal communication). By analyzing the Knolls Core interpretation, the Little Valley cycle is present at approximately 16.8 m from the top of the core. Given that the pit wall at Clive was 6.1 m high and does not capture the Little Valley cycle, it is possible that that other smaller lake cycles occurred in the Clive region in addition to the three intermediate lake events noted in Table 3

(labeled as Pre-Bonneville Lacustrine Cycles). There are few data to support the specific number of lakes that might have reached Clive, or the rate of sedimentation. There is also uncertainty associated with the particular times that these cycles occur, as age dating (e.g., via radiocarbon dating) has not been performed in the Great Salt Lake area. Most studies examine the degree of lake salinity using fossil records, and are associated with cores that are in or near the Great Salt Lake. For example, Balch et al. (2005; Fig. 6) estimated that there were six "saline/hypersaline" (i.e., shallow to intermediate) lake cycles that occurred between the Lake Bonneville and Little Valley cycles, and approximately that same number between the Little Valley cycle and the maximum age evaluated (300 ky). However, this work does not inform the question of whether these lakes may have reached the elevation of Clive, nor does similar work such as Davis (1998).

It is also possible that intermediate lakes could occur and reach the elevation of Clive under unusual conditions not necessarily associated with a return to a glacial cycle. The areal extent of lakes is not only determined by elevation, but also by local topography, precipitation, temperature, characteristics of inflow and outflow sources, and other factors. For instance, the Great Salt Lake 'spilled' over a 1285-m (4217-ft) amsl topographic barrier to the west of the present lake into the area of the present Great Salt Desert as recently as the 1700s (Currey et al., 1984). This expanded lake was about 15 m lower than the Clive site—a bit higher than the current surface elevation of the Great Salt Lake. Precise dating of shorelines for the Great Salt Lake and variants is unfortunately lacking. Radiocarbon dating for the Pyramid Lake area in Nevada indicates that this lake's levels have lowered approximately 35 m from the late Holocene Epoch (3.5 to 2.0 ky) to today (Briggs et al., 2005). Radiocarbon and tree-ring dating to determine lake levels in the Carson Sink area in Nevada indicates that lake elevations have risen approximately 20 m twice in the last 2000 years (Adams, 2003). It is not possible at this time to interpolate from these studies to the Great Salt Lake area. However, given the lack of empirical evidence that under present climate conditions an intermediate lake would reach the Clive site, this condition is not addressed. Future intermediate lake assumptions are described in Section 4.2.1.

Table 3. Lake cycles and sediment thickness from Clive pit wall interpretation (C. G. Oviatt, personal communication) [1]

lake cycle	thickness of sediment layer (m)	depth below ground surface (m)
Gilbert Lake transgressive/regressive phase[1]	1.05	1.05
Lake Bonneville Regressive Phase (reworked marl)	0.43	1.48
Lake Bonneville Open Water (white marl)	1.29	2.77
Lake Bonneville Transgressive (littoral facies)	0.76	3.53
Pre-Bonneville Lacustrine Cycle 3 (possible shallow lake)	0.71	4.24
Pre-Bonneville Lacustrine Cycle 2 (possible shallow lake)	0.62	4.86
Pre-Bonneville Lacustrine Cycle 1 (possible shallow lake)	1.14	6.00

[1] The upper sedimentary sequence is no longer interpreted as a Gilbert Lake phase (Oviatt, 2014) and may be surficial aeolian deposits and soils (Oviatt, personal communication, April, 2014).

3.4 Sedimentation

The types of sediment resulting from the formation and long-term presence of lakes in the Bonneville Basin are genetically diverse and can be divided into three components (Schnurrenberger et al., 2003): 1) chemical sediment (inorganic materials formed within the lake), 2) biogenic sediment (fossil remains of former living organisms), and 3) terrigenous or clastic sediments (grains and clasts that are mechanically and chemically fragmented from existing material, transported and deposited by sedimentary processes). A fourth type of associated sediment, not formed by lakes, includes aeolian deposits consisting of windblown grains of sand, silt or dust (loess). These deposits can locally be interbedded with lake sediments and may be affected by soil-forming processes (pedogenesis) during prolonged periods of subaerial exposure (land surface). All four types of sediments can be intermixed by lake-wave action or bioturbation, and deposited as clastic sediments during transgressive and regressive lake cycles.

During all pluvial lake cycles, evaporites are deposited, as well as carbonates in the form of tufas, marls, and mudstones. These sediments may contain varying components of shells (e.g. of mollusks), and ostracodes (Hart et al., 2004). Terrigenous sedimentation however, accounts for the major thickness of sediment observed throughout the sediment core record (C.G. Oviatt, personal communication). The geomorphological evidence in the form of depositional and erosional landforms produced at lake edges (lake shorelines) are carved into the landscape in the Bonneville Basin and provide examples of the erosional capacity of lake systems over long time periods. Given the difficulty in separating chemical, biogenic, and terrigenous sediment deposits in cores and natural exposures, the estimates reported below are assumed to be representative of cumulative sedimentation from all causes during a lake event.

Brimhall and Merritt (1981) reviewed previous studies that analyzed sediment cores of Utah Lake, a freshwater remnant of Lake Bonneville that formed at approximately 10 ka. They suggest that up to 8.5 m of sediment has accumulated since the genesis of Utah Lake, implying an average sedimentation rate of 0.85 mm/y or 850 mm/ky. Within the Bonneville Basin as a whole the major lake cycles resulted in substantial accumulations of sediment based on the depth of the cores analyzed (e.g., a 110-m core that corresponds to the past 780 ky, or four deep lake cycles [Oviatt et al., 1999]), which averages about 140 mm/ky. Einsele and Hinderer (1997) indicate that sediment accumulation in the Bonneville Basin occurred at a rate of 120 mm/ky during the past 800 ky. The Knolls Core suggests that there has been 16.8 m or sediment formed in the last glacial cycle, or nearly 170 mm/ky.

Interpretations of the Clive pit wall (C.G. Oviatt, unpublished data) indicate that the sedimentation rate at the Clive site for the Lake Bonneville cycle is on the order of 2.75 m over a 17- to 19-ky time period (140 to 160 mm/ky). By contrast, shallow lacustrine cycles that occurred prior to Lake Bonneville (but after the Little Valley cycle) indicate that the amount of sediment deposited during each cycle is approximately 1/3 that of the Bonneville sediment deposited. The timing of these shallow lake cycles is uncertain, however it can be approximated when comparing the Clive pit wall interpretation to the Knolls Core (C.G. Oviatt, personal communication). The Little Valley lake cycle is exhibited in the Knolls Core at a depth of approximately 17 m, which is roughly 14 m deeper than the beginning of the transgressive phase of the Bonneville lake cycle event noted on the Clive pit wall interpretation. Given the Little

Valley event occurred 150 ka, a sedimentation rate can be approximated for the depth between this event and the transgressive phase of the Bonneville cycle of 110 mm/ky.

These data support greater sedimentation rates in shallow lakes (sedimentation in Utah Lake is much greater, and sedimentation in the Clive Pit Wall indicates lower rates for a deep lake cycle), but also suggest that the sedimentation rate in each glacial cycle is similar.

There is no information available that addresses aeolian deposition rates during a 100-ky cycle, partly because any aeolian deposition is inter-mixed with all other forms of sedimentation from intermediate and deep lakes.

4.0 Conceptual Overview of Modeling Future Lake Cycles

As stated in the Conceptual Site Model (Neptune, 2011a), there is a lack of peer-reviewed literature that allows accurate and precise prediction of the direct effects of future climate change on major lake formation in the Bonneville Basin. However, assuming no major changes from recent climate cycles, the probability of another major lake cycle occurring in the Bonneville basin within the next few million years is high. Variations in the Earth's orbital parameters in combination with increases in inputs of freshwater into the oceans are likely to lead to another major ice age and could alter long-term climatic patterns in the Bonneville Basin, resulting in deep lake formation. It is possible that the Clive site will be subjected to deep lake formation in the future, unless anthropogenic effects on atmospheric CO_2 concentrations cause major changes in climatic patterns (Berger and Loutre, 2002).

The basic intent of the deep-time model is to allow lakes to recur that are sufficiently large that the above-ground portions of the Federal DU Cell will be obliterated, and so that the sedimentation rates for each glacial cycle are similar. The exact timing of the recurring lakes is not important, the current 100-ky cycle excepted. The deep-time model allows the possibility of a deep lake to return in each 100-ky cycle. It also allows intermediate lakes to recur at a frequency that allows the 100-ky sedimentation rate to be satisfied. The current 100-ky cycle is not modeled explicitly. It is possible that the current interglacial period will last for another 50 ky, which is unusually large compared to the interglacial period for recent 100-ky ice age cycles.

The return of a deep lake is assumed to cause the above-ground features of the site to be obliterated, and the contents of the waste embankment to be dispersed through wave action. All of the DU waste, including portions disposed below present-day surrounding grade, is conservatively assumed to mix with lake sediments. Each new lake event causes more sedimentation, which will either bury or continually mix the waste with more sediment over time. This basic conceptual model is described in more detail below. The assumption of complete erosion of the embankment during the first lake return to the Clive site is a simplifying and conservative assumption. Figure 12 in the Clive DU PA Model final report v1.2 and the accompanying text show that the ^{238}U concentration in sediments is driven by the first lake event, with decreasing sediment concentrations in successive lakes. If the embankment is not

completely eroded, there will be less waste mixed in the sediments, and lower sediment concentrations of ^{238}U in the first and all successive lake sediments.[3]

4.1 Future Scenarios

Various Features, Events, and Processes, and (FEPs) may be associated with the effect of a lake return scenario on the Federal DU Cell, including wave action, sedimentation, and site inundation. Details of the FEPs process are provided in the *Features, Events and Processes for the Clive DU Performance Assessment* report (Neptune, 2014b). Starting with current conditions, representative lake occurrence scenarios for the long-term future are described below and depicted in Figure 3. Note that there are two components of the models used to represent these scenarios. The first is modeling lake formation and dynamics, based upon the scientific record. The second is modeling the fate of the Federal DU Cell.

[3] Note that the Deep Time component of the Clive DU PA Model v1.2 assumes that the DU waste is dispersed upon the return of a lake of sufficient elevation to destroy the site, as was assumed in v1.0. However, if the waste is configured to be disposed below grade (in the five bottommost waste layers) it is extremely unlikely that any of the DU waste would be so dispersed. Note also that aeolian deposition will occur during the inter-glacial period, and this will cause the elevation of grade to be raised, making it even more unlikely that DU waste buried below current grade would be so dispersed, and providing additional site stability.

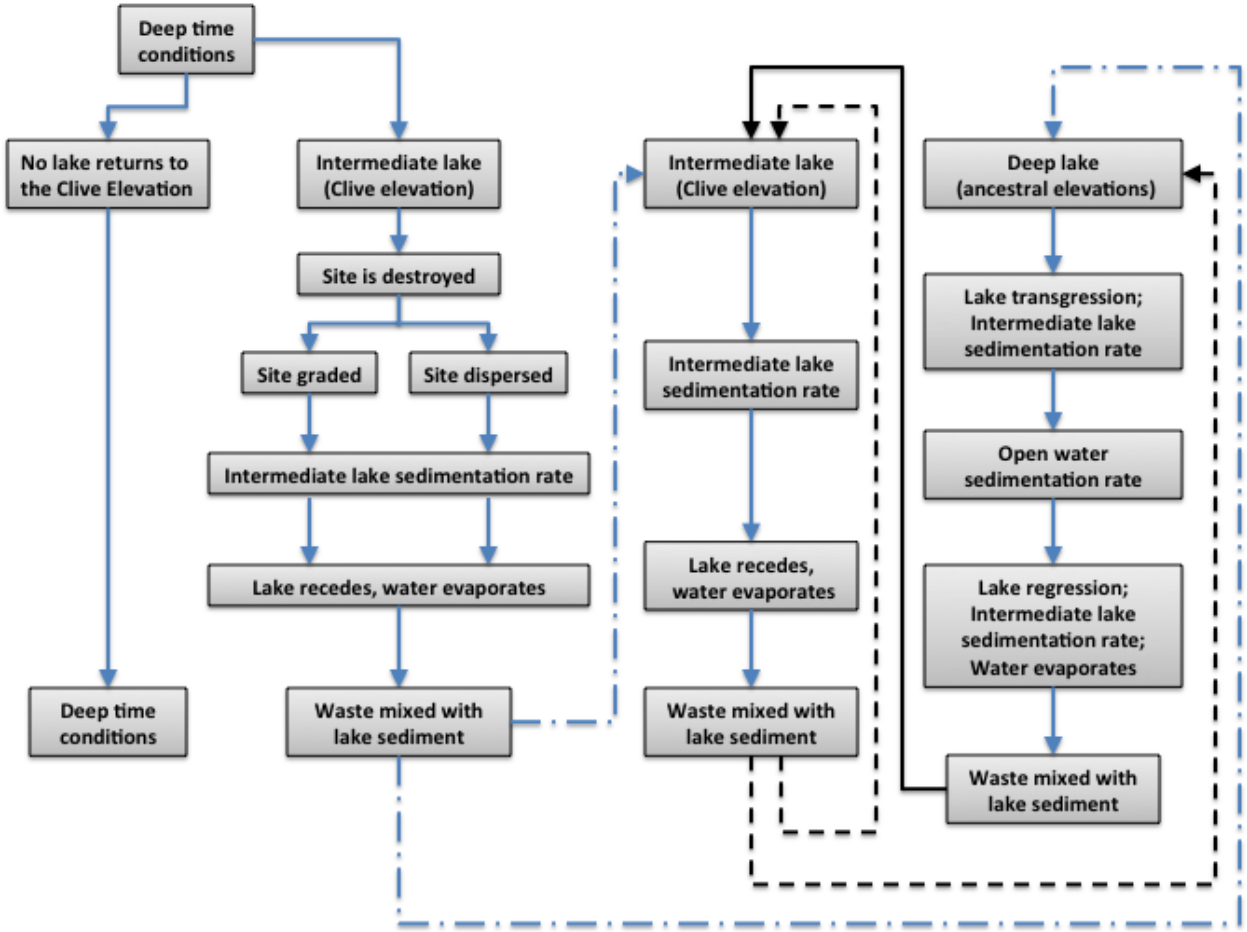

Figure 3. Scenarios for the long-term fate of the Clive facility[4]

The Great Salt Lake represents the current condition of a shallow lake in the Bonneville Basin. Lakes such as this are likely to exist in all future climatic cycles, but lakes that do not reach the elevation of the DU waste embankment at Clive will not affect the waste embankment. For the Clive DU waste PA model, it is assumed that destruction of the waste embankment will result from the effects of wave action from an intermediate or deep lake. In effect, it is assumed that a lake is large enough that obliteration of a relatively soft pile will occur. This assumption separates shallow and intermediate lakes. In this obliteration scenario, all of the embankment material above grade is assumed to be dispersed through a combination of physical dispersal through wave action and dissolution into the water column above the waste dispersal area[5]. Waste material that dissolves into the lake eventually returns to the lake bed through precipitation or evaporation as the lake regresses.

[4] The scenario that indicates that no lake returns to the Clive elevation implies that a shallow lake is present and never reaches the Clive site.

[5] See footnote 4.

Assuming DU waste is dispersed as part of the disposal system[6] while the lake is present, some waste in the water column will bind with carbonate ions and precipitate as chemical and biogenic sediment, while the eroded insoluble waste will remain within the clastic sediment as the lake eventually recedes. Wave action during the lake recession is expected to rework and mix the chemical, biogenic and clastic lake deposits. The combined complexity of processes affecting the compositional and sedimentary features of lacustrine deposits (Fritz, 1996) and the mixing of lake sediments during regressive and transgressive lake cycles makes it difficult to develop quantitative models of chemical and physical processes affecting the distribution of waste radionuclides in lake waters and sediments. Instead, the model makes two conservative assumptions: First, all dissolved waste remains within the local water column and is re-precipitated into the lake sediments during lake regression. Second, clastic sediments mixed with waste material remains within the vicinity of the Clive site. In reality, waste radionuclides dissolved in lake waters will mix and be diluted by lake circulation driven by prevailing winds and geostrophic balances (Jewel, 2010). Waste-sediment mixes will be dispersed by wave action and long shore drift. Sediment concentrations decrease over time because the amount of waste does not change other than through decay and ingrowth, whereas more sediment is added over time.

The model assumes the waste is fully mixed with the accumulated sediment, whereas in reality some waste might be buried beneath the level of future wave action during successive lake cycles. The model also allows large dispersal areas, and maintains a water column for accepting dissolved waste radionuclides through dissolution that is limited to a projection above the dispersal area. As noted above, these assumptions are conservative, and allow for greater concentrations of waste remaining at the eroded Clive site. The conservatism is included in this model because of the difficulty of developing realistic models and the lack of data to quantify the model processes. For example, the extent of mixing of previous sediment with new sediment is difficult to constrain, hence an assumption that the sediments completely mix is expedient, but conservative. An approach that considers the size of the spits from the Grayback Hills north of the Clive facility that were formed during the lake event might provide a better analog. It should be noted that a Gilbert-sized lake would not reach the Clive elevation (Oviatt, 2014). The depth of a lake in the Clive DU PA Model that is needed to obliterate the waste embankment can be as shallow as 1 m, which may or may not have sufficient wave power to obliterate the site. Dissolution into such a shallow lake might over-estimate lake water concentrations, if such a shallow lake cannot obliterate the waste embankment. There are various reasons why the deep time model might over-estimate lake water and sediment concentrations, but the data needed to better specify the model are not readily available. Depending on the model performance, data collection in support of model refinement with reduction of conservative assumptions might prove to be desirable.

One other factor that is important for this model is that the lake formation model is applied to each 100-ky cycle similarly: The current 100-ky cycle is not treated differently, despite evidence that the current interglacial period might last for another 50 ky (Berger and Loutre, 2002). In the model, therefore, an intermediate lake can return sooner than might be expected in the current 100-ky cycle. From the perspective of obliteration of the embankment, the timing is largely

[6] This assumption is made in the Clive DU PA Model v1.2 – see footnote 4.

irrelevant. The mass of waste does not change much over time. However, the deep-time model also assumes that the form of DU available for deep-time transport is U_3O_8, which is far less soluble than UO_3 (see *Radioactive Waste Inventory for the Clive PA* (Neptune, 2011c)). The "deconverted" DU waste from the gaseous diffusion plants consists primarily of U_3O_8, but the DU waste from the Savannah River Site is UO_3. Fate and transport modeling performed in the Clive DU PA Model indicates that most of the more soluble UO_3 will have migrated to groundwater within 50 ky. Consequently, the deep time model focuses on U_3O_8 as the form of DU available for deep-time migration.

The remainder of this section describes the specifics of the models that have been developed for this analysis, including lake formation and sedimentation.

4.2 Intermediate and Deep lake Formation

This scenario assumes that changes in climate will continue to cycle in a similar fashion to the climate cycles that have occurred since the onset of the Pleistocene Epoch. These changes follow those observed in the marine oxygen isotope record (Figure 2). The record captures major climate regime shifts on a global scale and is used in this scenario in conjunction with expert opinion (C.G. Oviatt, personal communication) and site-specific sediment core and pit wall information to determine the approximate periodicity of lake events. However, uncertainties exist due to the limitations related to the quality of the sediment core data. The following subsections provide more detail with respect to the assumptions for both intermediate and deep lake formation.

4.2.1 Intermediate Lake Formation

The Great Salt Lake represents the current condition of a lake in the Bonneville Basin. Lakes such as this are likely to exist for periods of time during all future climatic cycles, but lakes that do not reach the elevation of the DU waste embankment at Clive will not affect the Federal DU Cell, so they need not be modeled explicitly. However, it is assumed that during the 100-ky climatic cycles, larger lakes will occur, including lakes that reach the elevation of Clive. Although a definitive distinction is not made, lakes that reach the elevation of Clive but do not develop into a deep lake are considered intermediate lakes. These intermediate lakes are also assumed to be large enough that their wave action will destroy the waste embankment. Intermediate lakes might occur during the transgression and regression of a deep lake, or might occur during a glacial cycle that does not produce a deep lake, perhaps in conjunction with glacial cycles that are shorter and less severe than the 100-ky year glacial cycles previously discussed (for example, potentially the current 100-ky cycle).

In general, variation in lake elevation is assumed to occur at all lake elevations. The variation is due to local temporal changes in temperature, evaporation and precipitation. For example, the Great Salt Lake has seen elevation changes of several tens of feet in the past 30 to 40 years. In addition, the Great Salt Lake has seen greater elevation changes in the past 10 ky, but in no cases since the Younger Dryas has the Great Salt Lake reached the elevation of Clive.

Sedimentation is assumed to occur during these intermediate lake events at greater annual rates than is assumed to occur for the open-water phase of deep lakes. This is based on the pre-Bonneville lacustrine cycles that are documented in Table 3 (Clive pit wall interpretation – see Appendix A). The lake is assumed to recede after some period of time, at which point a shallow

lake relative to the Clive facility will occupy Bonneville Basin until the next intermediate or deep lake cycle. The details relating to the mathematical approach employed to model this scenario and model parameters are provided in Section 29.

4.2.2 Deep Lake Formation

In this scenario, a deep lake forms throughout the Bonneville Basin in response to major glaciation in North America and the Northern Hemisphere, following the ongoing 100-ky glacial cycle. Increases in precipitation and decreases in evaporation over the long term, and subsequent increases in discharge to the Bonneville Basin via rivers that drain high mountains along the eastern side of the basin in general have resulted in lakes that are more than 30 m deep and cover an area similar to that of the most recent pluvial lake episode (e.g., Lake Bonneville, Provo Shoreline). This same extent of lake formation is assumed to occur in the future. Under such a scenario, the depth of a lake at the location of the Clive facility could be many tens of meters, resulting in sedimentation over the long period of time of the lake's existence. A key difference between this scenario and the intermediate lake scenario is that both the transgressive and regressive phases of lake formation are considered. Transgressive and regressive phases of lake formation can lead to brief periods of rising and falling water levels in both phases. These phases of transgression and regression are also assumed to have higher sedimentation rates than the open-water phase. Upon the complete regression of a deep lake, it is assumed that only intermediate lakes will form until the deep lake associated with the next 100-ky climate cycle occurs. It is assumed that destruction of the waste embankment occurs in response to the formation of a deep lake, if the first deep lake occurs prior to formation of an intermediate lake.

5.0 A Heuristic Model for Relating Deep Lakes to Climate Cycles from Ice Core Temperature

In this section, a model is presented for estimating lake elevation that uses surface temperature deviations from the EPICA Dome C ice core data (Jouzel et al., 2007). The model is not intended to be highly accurate, but rather is aimed at capturing the major lake-cycle features as shown in the studies conducted by Oviatt et al. (1999), Link et al. (1999), and the sediment core and pit wall interpretations (C.G. Oviatt, personal communication). This model is not used as a predictive model but rather to form a basis for the character and dynamics of lake events, which will be implemented in the deep time model developed in Section 29.

The deep-sea benthic $\delta^{18}O$ record is in excellent agreement with the EPICA Dome C deuterium measurements for the last ~810 ky (Jouzel et al., 2007). Temperature anomaly data for the past 810 ky were obtained from the World Data Center for Paleoclimatology, National Oceanic and Atmospheric Administration/National Climate Data Center. These data are made available based on calculations described in Jouzel et al. (2007), and are plotted in Figure 4. From the 810 ky of data, the temperature deviations range from $T_{min} = -10$ºC to $T_{max} = +5$ºC. This range is used to bound extreme events.

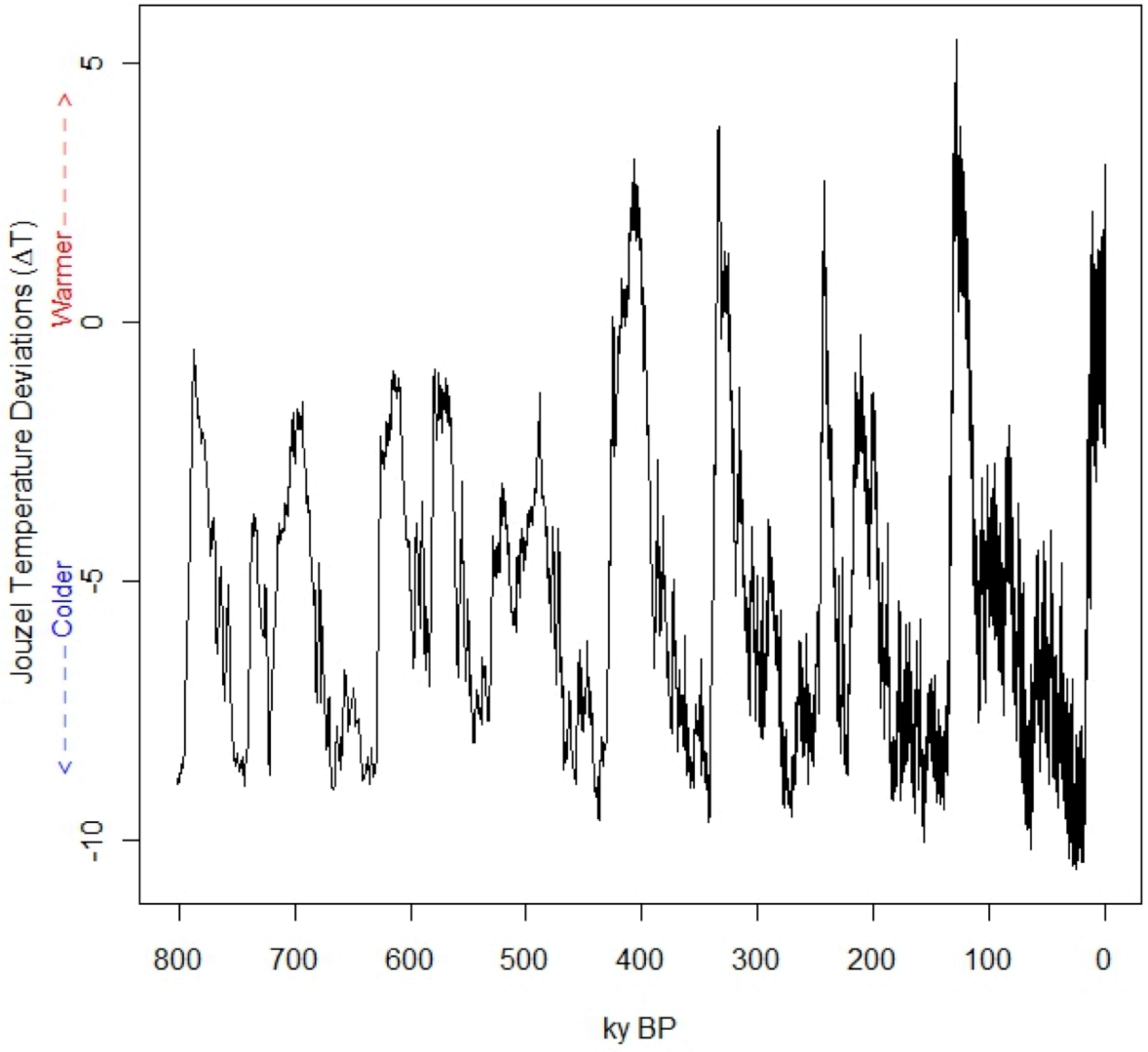

Figure 4. Temperature deviations for the last 810 k (from Jouzel et al., 2007)

5.1 Conceptual Model

Water balance in the Bonneville Basin is affected by many complex processes, so modeling water balance simply as a function of temperature alone is not expected to produce any precise results, but might succeed in representing a coarse feature. The conceptual model is based on a water balance reservoir model of precipitation versus evaporation. If precipitation outpaces evaporation, the lake elevation increases. If evaporation outpaces precipitation, then the lake elevation decreases. Precipitation and evaporation are affected directly by temperature, but long-term patterns of precipitation are affected more greatly by the presence or absence of continental

glaciation in North America. Thus, glaciation is modeled first using a simple reservoir model depending on temperature.

5.2 Glaciation

The water balance model begins by constructing a "continental glacier" – an artificial construct that represents a glacier large enough to affect precipitation levels in the Bonneville Basin. The extent of glaciation in proximity to the Bonneville Basin is assumed to be zero initially, which is a reasonable approximation for the start time of 785 ka, a start time chosen because it corresponds to a warmer climate phase (data from Jouzel, et al., 2007; see Figure 4). For each time step of 500 years, an increase in glacial magnitude is dependent on temperature deviation (ΔT) as scaled in Jouzel (see Figure 4):

$$Glacial_{addition}(\Delta T) = \begin{cases} 0 & \text{if } \Delta T \geq \Delta T_{GMax} \\ \frac{1}{N_{GA}}(e^{R_{GA}\cdot\Delta T_{GMax}-\Delta T} - 1) & \text{if } \Delta T < \Delta T_{GMax} \end{cases} \quad (1)$$

where

- N_{GA} is a normalizing constant:

$$N_{GA} = e^{R_{GA}\cdot(\Delta T_{GMax}-\Delta T_{\min})} \quad (2)$$

- R_{GA} is a rate parameter (yr^{-1}), and
- T_{GMax} is a threshold temperature (degrees Celsius).

Since the glacier is an artificial construct for modeling purposes, the units and scale of the glacial "magnitude" are arbitrary. The parameters of the precipitation model described below must be calibrated appropriately to the scale of the glaciation model.

For each time step, the decrease in glacial magnitude is also modeled as a function of temperature:

$$Glacial_{subtraction}(\Delta T) = \begin{cases} 0 & \text{if } \Delta T \leq \Delta T_{GMin} \\ \frac{S_{GS}}{N_{GS}}(e^{R_{GS}\cdot\Delta T-\Delta T_{GMin}} - 1) & \text{if } \Delta T > \Delta T_{GMin} \end{cases} \quad (3)$$

where

- N_{GS} is a normalizing constant:

$$N_{GS} = e^{R_{GS}\cdot(\Delta T_{max}-\Delta T_{GMax})} \quad (4)$$

- R_{GS} is a rate parameter (yr^{-1}), and
- T_{GMin} is a threshold temperature (degrees Celsius).

The change in glacial magnitude for a time step is thus:

$$Glacier_t = max[0, Glacier_{t-1} + Glacial_{addition}(\Delta T_t) - Glacial_{subtraction}(\Delta T_t)] \quad (5)$$

where the *t* subscript is a time step index. The time step used for the model is 500 years.

The parameters of the model were calibrated heuristically to compute parameters that produced a glacial cycle that appeared reasonable for this coarse model. The set of parameters computed was:

$$\begin{aligned} \Delta T_{GMax} &= -6 \\ R_{GA} &= 0.25 \\ \Delta T_{GMin} &= -6.0 \\ R_{GS} &= 0.2 \\ S_{GS} &= 5.0 \end{aligned} \tag{6}$$

The change in the glacial magnitude for a particular time step as a function of temperature is shown in Figure 5. These values lead to slow growth during the very cold phases (Jouzel temperature deviations of less than –6°C) of the glacial cycle, and rapid recession during warm phases (Jouzel temperature deviations of greater than –6°C).

5.3 Precipitation

A coarse model for precipitation in the Bonneville Basin was developed dependent on global temperature (as precipitation generally increases with global temperature), lake surface area (which affects recharged evaporation), and an additional effect that depends of the magnitude of the continental glacier. The precipitation in meters of annual rainfall is modeled as:

$$P_t(\Delta T_t, L_{t-1}, G_{t-1}) = B_P + R_{PT} \cdot \Delta T + R_{PLSA} \cdot SA(L_{t-1}) + S_{PG} \cdot e^{R_{PG} \cdot G_{t-1}} \tag{7}$$

where

B_P	is a baseline precipitation,
R_{PT}	is a coefficient of linear effect of global temperature,
R_{PLSA}	is a coefficient of linear effect of the surface area of the lake, and
$SA(L)$	is the surface area in km^2 associated with lake elevation L.

The effect of temperature and lake surface area are modeled as linear, while the glacial effect is exponential with respect to glacier size. The set of parameters calibrated to the glacial magnitude model are:

$$\begin{aligned} B_P &= 0.30 \\ R_{PT} &= 0.005 \\ R_{PLSA} &= 2\times10^{-6} \\ S_{PG} &= 0.06 \\ R_{PG} &= 0.03 \end{aligned} \tag{8}$$

The precipitation is then converted to a volume by multiplying by the area of Bonneville Basin (approximately 47,500 km^2).

5.4 Evaporation

Evaporation rate in the region is modeled as a function of temperature:

$$E_t(\Delta T_t) = B_E + \frac{S_E}{N_E} \cdot e^{R_E \cdot (\Delta T - \Delta T_{min})} \tag{9}$$

where $N_E$is a normalizing constant:

$$N_E = e^{R_E \cdot (\Delta T_{max} - \Delta T_{\min})} \tag{10}$$

The evaporation is then converted to a volume by multiplying by the area of the basin.

The calibrated parameters are:

$$\begin{aligned} B_E &= 0.32; \\ S_E &= 0.3 \\ R_E &= 0.05 \\ \Delta T_{min} &= -10 \\ \Delta T_{max} &= 5 \end{aligned} \tag{11}$$

If the precipitation volume exceeds the evaporation volume, then the difference is added to the lake volume, and the lake elevation is calculated from the total lake volume.

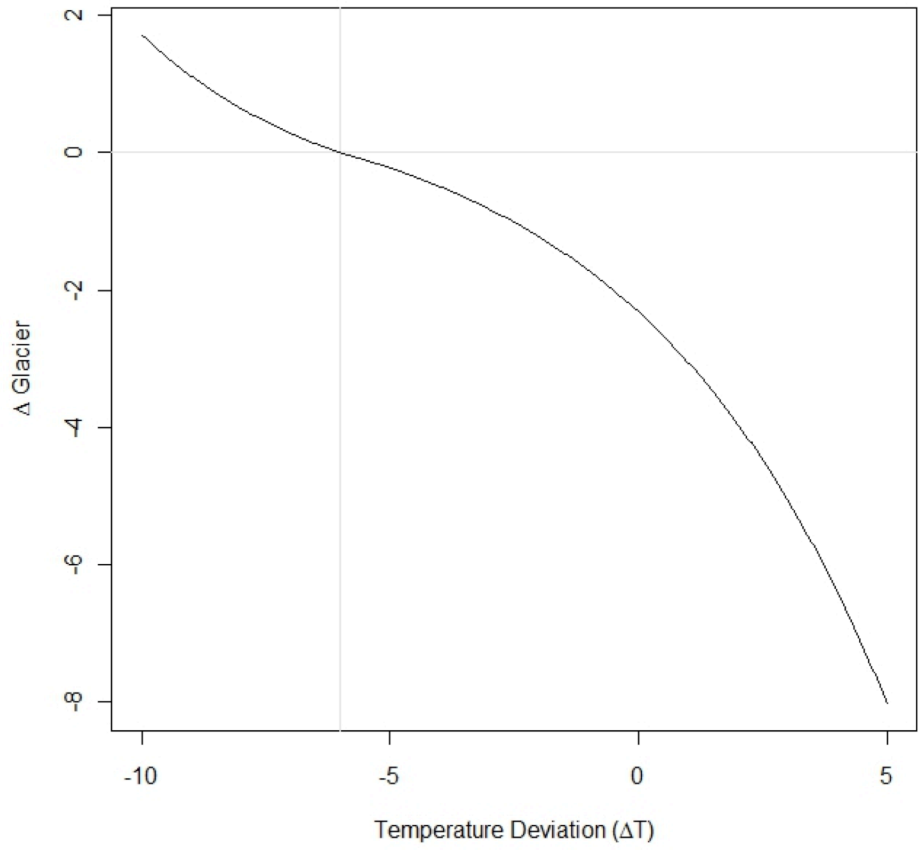

Figure 5. Glacial change as a function of temperature for the coarse conceptual model

If the evaporation volume is greater than the precipitation volume, then the total evaporation is adjusted downward to adjust for the actual surface area exposed (rather than the full surface area of the basin as used in the initial calculation). The difference between the adjusted evaporation and the precipitation is then subtracted from the lake volume, and the lake surface elevation is calculated from the total lake volume.

$$\Delta Volume_t = \begin{cases} [P_t \Delta T_t - E_t(\Delta T_t)] \cdot SA_{basin} & \text{if } E_t(\Delta T_t) < P_t(\Delta T_t) \\ [P_t \Delta T_t - E_t(\Delta T_t)] \cdot \dfrac{SA(L_{t-1})}{SA_{basin}} & \text{if } E_t(\Delta T_t) \geq P_t(\Delta T_t) \end{cases} \quad (12)$$

5.5 Simulations

For simplicity, the lake volume and glacial magnitude are assumed to be zero at the first time step (785 ka), as that time step corresponds to a warm climate phase. The values for the parameters given above are calibrated graphically to produce reasonable precipitation versus evaporation values. Several lake elevation histories were simulated by simulating the parameter

values of the model probabilistically. The distributions for the parameters were lognormal with medians equal to the parameter values listed in Equations (6), (8), and (11). The simulations provide a variety of behaviors depending on the combination of parameters simulated.

A few common features are apparent in the simulated results. The largest lakes tend to occur at the times of Lake Bonneville, Little Valley, and Lava Creek, and the smallest 100-ky cycle lake occurs in δO^{18} cycle 14 (~533 ka), which matches the scientific record. When the simulated glaciation effects are small (R_{GA} and R_{GS}), precipitation change in the model is due primarily to temperature change. In this case, deep lakes form with few intermediate lakes, as the lake elevation history in the top graph in Figure 6 shows. When glaciation effects are larger, then deep lakes tend to last longer, and intermediate lakes form, as the lake elevation history in the lower graph of Figure 6 shows.

The simulation models were then calibrated further by combining the simulated lake histories with sedimentation rates seen in sediment cores. Based on the results of this coarse model calibration, some assumptions are carried forward to the deep time model.

1. The 100-ky cycle in global temperature is a strong indicator of the return of a deep lake. While not all simulations showed a lake returning to the Clive elevation in every 100-ky cycle (particularly δO^{18} cycle 14), the results were consistent enough to treat as systematic behavior for a heuristic model.

2. Intermediate lakes should be a part of the deep time simulation, because sedimentation rates did not calibrate well with simulations that produce only deep lakes.

3. Intermediate lakes are more likely to occur in the later stages of the 100-ky cycle than in the early stages, primarily in conjunction with the slowly decreasing temperatures across the cycle (as opposed to the relatively rapid warming period that occurs at the end of a 100-ky cycle).

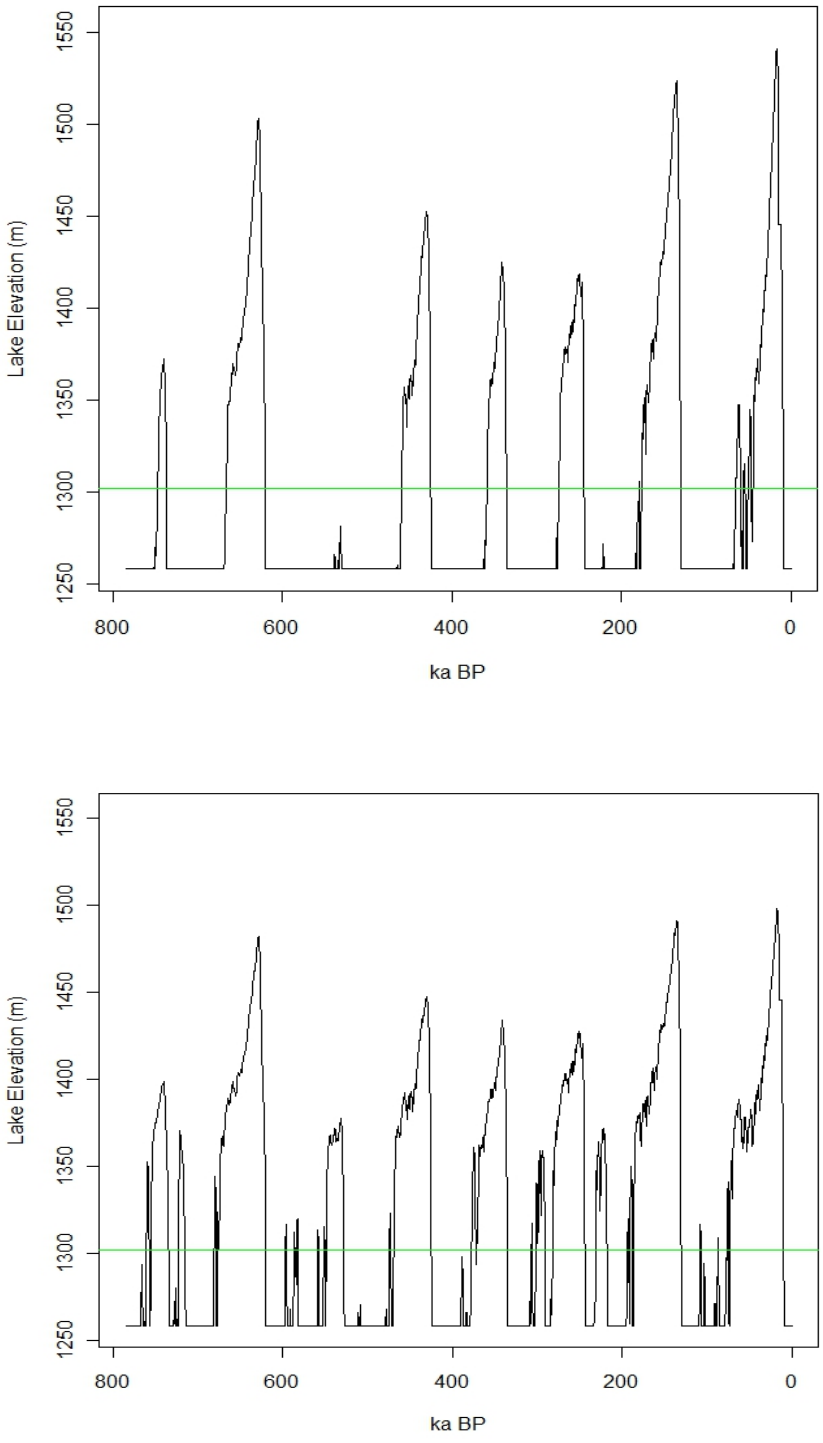

Figure 6. Two example simulated lake elevations as a function of time, with Clive facility elevation represented by green line

6.0 Modeling Approach for the PA Model

Depleted uranium, since it is primarily ^{238}U, has the property of becoming more radioactive with time, due to the ingrowth of decay products that were separated out during processing. The extremely long half-life of ^{238}U regulates this ingrowth, and the DU waste gets more radioactive over a period of about 2.1 My, and remains at that constant activity for billions more years. It is therefore of interest to understand, at least at a qualitative level, what the distant future (beyond 10 ky) holds for the Clive facility. This deep time modeling includes what might be expected over those 2.1 My, in a stylized depiction of the effects of lakes returning to the Bonneville Basin.

With the return of the first lake that inundates the site, contaminant transport modeling within the embankment ceases, and those above-ground portions of the facility are assumed to be obliterated and mixed with lake sediments. While the lake is present, the dispersal of the disposed inventory is coincident with dissolution of wastes into the water column, and their burial under fresh lacustrine sediments. Modeling the details of such processes is beyond the scope of this PA, but gross estimates of radionuclide concentrations in sediments and in the lake water are made. The long term concentrations of long-lived isotopes and their decay products are of primary concern. A detailed, precise model of temporal lake cycles is therefore not necessary—rather, a model that captures the major features of lake recurrence is indicated. The basic features of the heuristic lake formation model presented in Section 21 are abstracted into the Clive DU PA Model to construct a probabilistic model for the deep time model. The various components of this model are presented here.

6.1 Deep Lakes

The 100-ky climate cycle is treated as a sufficiently robust effect to create a hypothetical lake that will reach and exceed the elevation of Clive each cycle. The exact time of occurrence is not a crucial parameter, due to the slowly-changing concentrations during deep time. Thus, the lake is set to be present at each 100-ky mark, with time beginning at 10 ky (the end of the quantitative performance period addressed for the quantitative dose assessment component of the PA).

There is little information on the amount of time that the Clive location has been under water. Lake Bonneville has been estimated to have been present at the elevation of Clive for a duration of approximately 16 ky (Oviatt et al., 1999). Durations of older deep lakes are unknown. Thus, a conservative choice was made to allow deep lakes to endure an average of about 20 ky (conservative in the sense that more waste will migrate into the water column). The occurrence time for each deep lake is set by choosing a start time some number of years prior to the 100-ky mark. The start time is represented by a lognormal distribution with geometric mean of 14 ky prior to the 100-ky mark, and a geometric standard deviation of 1.2. The end time is represented by a lognormal distribution with geometric mean of 6 ky after the 100-ky mark, and a geometric standard deviation of 1.2. These distributions are depicted in Figure 7.

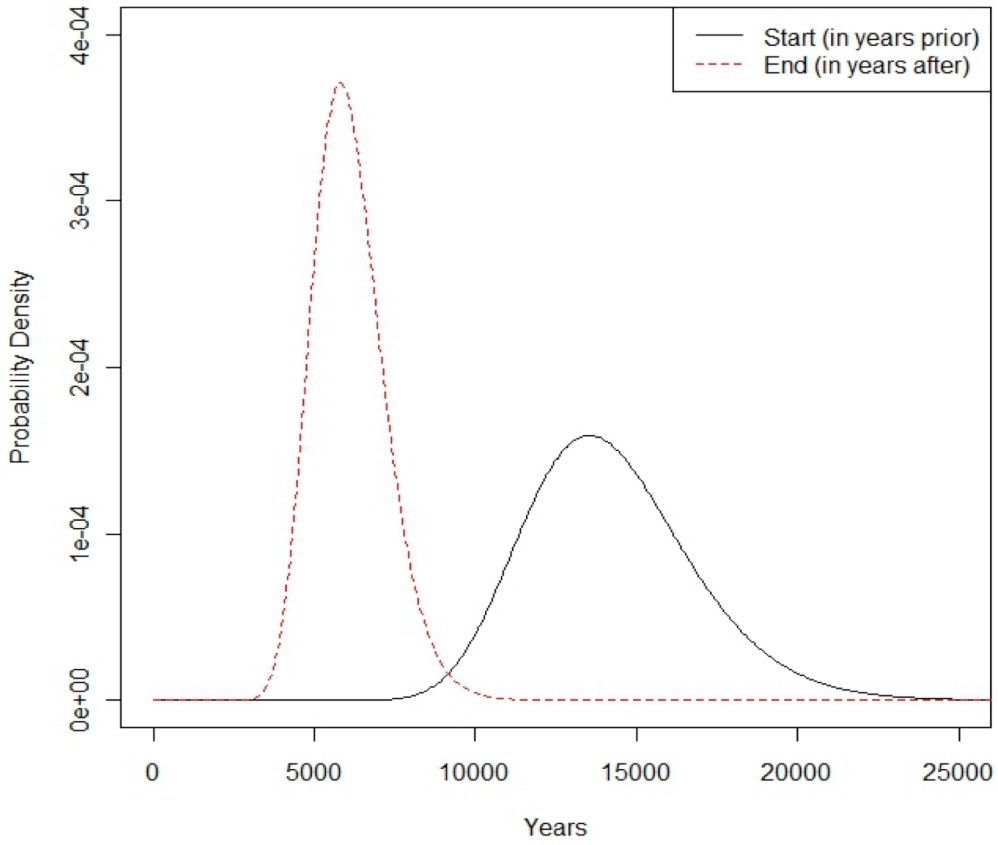

Figure 7. Probability density functions for the start and end times for a deep lake, in years prior to the 100-ky mark and years after the 100-ky mark, respectively.

6.2 Intermediate Lakes

Intermediate lakes are modeled as potentially occurring anytime between deep lake events. In order to reflect the slow decrease in temperature over the 100-ky cycle, the occurrence time for intermediate lakes is modeled as a Poisson process with a rate that increases linearly over the cycle time, from a rate of 0 to 7.5 lakes per 100 ky. This process produces an average of about 3 intermediate lakes per 100 ky. There is little recorded basis for this number, but it matches reasonably with the heuristic model of Section 21, and was chosen so that long-term sedimentation rates matched the average from previous lake cycles, as estimated from the sedimentation of individual lakes developed in Section 31.

There is virtually no information for the duration of intermediate lakes, due to the high mixing rate of shallow lake sediments, which makes dating of times within a single stratigraphic layer of a shallow lake sediment core extremely difficult. Thus, a distribution was chosen to roughly calibrate with the heuristic model: lognormal with geometric mean of 500 y and geometric standard deviation of 1.5.

6.3 Sedimentation Rates

Deposition of material in the area of the Clive facility is a continuous process that occurs during shallow, intermediate and deep lake periods. During shallow lake periods, as observed in present-day conditions, aeolian deposition of sand, silt and loess is the primary sedimentary mechanism. However, aeolian deposits are rarely observed in sediment cores, presumably because of reworking of the depositions during lake transgressions and mixing with lake-derived sediments. Note however that the upper part of the Clive pit is now interpreted to be of aeolian origin and soils have been described in the Burmester core indicating prolonged periods of subaerial exposure (Oviatt, personal communication, April 2014). Intermediate lake sediments include chemical, biogenic, and terrigenous sediments, with their proportions dependent on the size and duration of the lake and the interplay between deep lake deposition and near-shore sedimentary processes. Schofield et al. (2004) note that the large fetch of Lake Bonneville (distance of wave forming winds over the water) produced a variety of wave-dominated erosional and depositional sedimentary and geomorphic features. They identified cross-sections of erosion-dominated and deposition dominated shorelines and the composite sedimentation rates of shoreline profiles will be dependent on local process of wind/wave erosion and deposition and supply of sediments from alluvial fans flanking pluvial lakes (See Schofield et al., 2004; their Figs 3 and 4). Moreover, as noted previously, since aeolian depositional layers are not commonly observed in the sediment cores, the model effectively combines aeolian deposits with lake sediments. The mixing probably occurs during intermediate lake cycles, which are likely to be the first lakes after interglacial periods. These assumptions require that there is a mixing depth associated with each lake recurrence. However, the mixing process itself makes it very difficult to assign mixing depths for the different layers in the sediment cores; mixing depths are probably determined by the dynamics of wave activity and resulting erosion/deposition during lake transgressions and regressions.

Deep lakes, by contrast, have similar sediment deposition rates to intermediate lakes in their transgressive and regressive phases, but have different, slower, rates when the lake is deep enough that the dominant sedimentation process is precipitation of chemical and biogenic material. Records from the sediments cores are able to distinguish between layers associated with intermediate lakes with predominant sediment mixing , and sedimentary layers associated with a large deep lake that are dominated instead by chemical and biogenic deposition.

Based on the available data from the sediment cores, sedimentation rates are expected to be higher when lake water is shallow than when a deep lake covers the Clive site.

For deep lakes, a sedimentation rate is modeled as a lognormal distribution with geometric mean of 120 mm/ky and geometric standard deviation of 1.2, a distribution that covers the range of observed values for deep lakes described in Section 14. This distribution is represented in Figure 8. The sedimentation rate is applied for the simulated duration of the deep lake. In addition, sedimentation is added at the beginning of the lake cycle as well as the end that represents the shallow phase of the transgressive and regressive lakes. This additional sediment mimics the behavior of an intermediate lake.

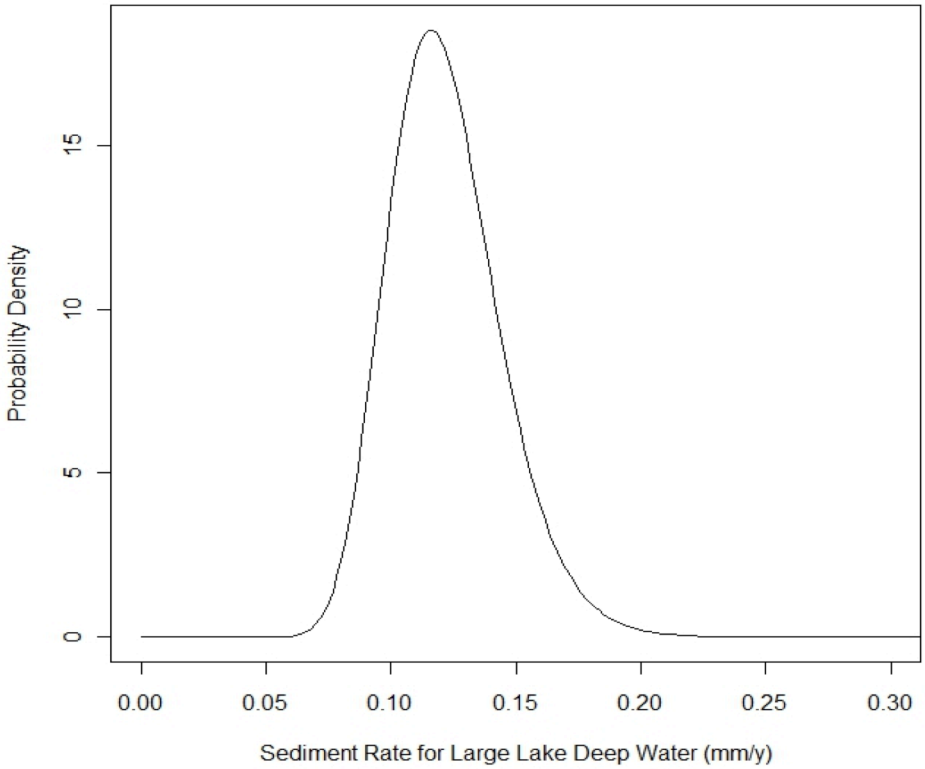

Figure 8. Probability density function for sedimentation rate for the deep-water phase of a deep lake

For intermediate lakes (and shallow phases of deep lakes), there is high likelihood of multiple short-term transgressions and regressions with respect to the elevation of Clive. For example, the Clive pit wall (Appendix A) shows three distinct lakes after the deep-water phase of Lake Bonneville and three distinct lakes prior to the deep-water phase of Lake Bonneville. Without further systematic study of a sediment cores and trench sections in and around the Clive site, including chronology studies, it is impossible to determine if these distinct lakes were separated by a few years or a few hundred years; i.e., whether they are distinct lake events or simply part of the transgression and regression of Lake Bonneville. However, based on current behavior of the lake, some year-to-year variation in the lake elevation occurs, in addition to the longer-term trends in lake elevation.

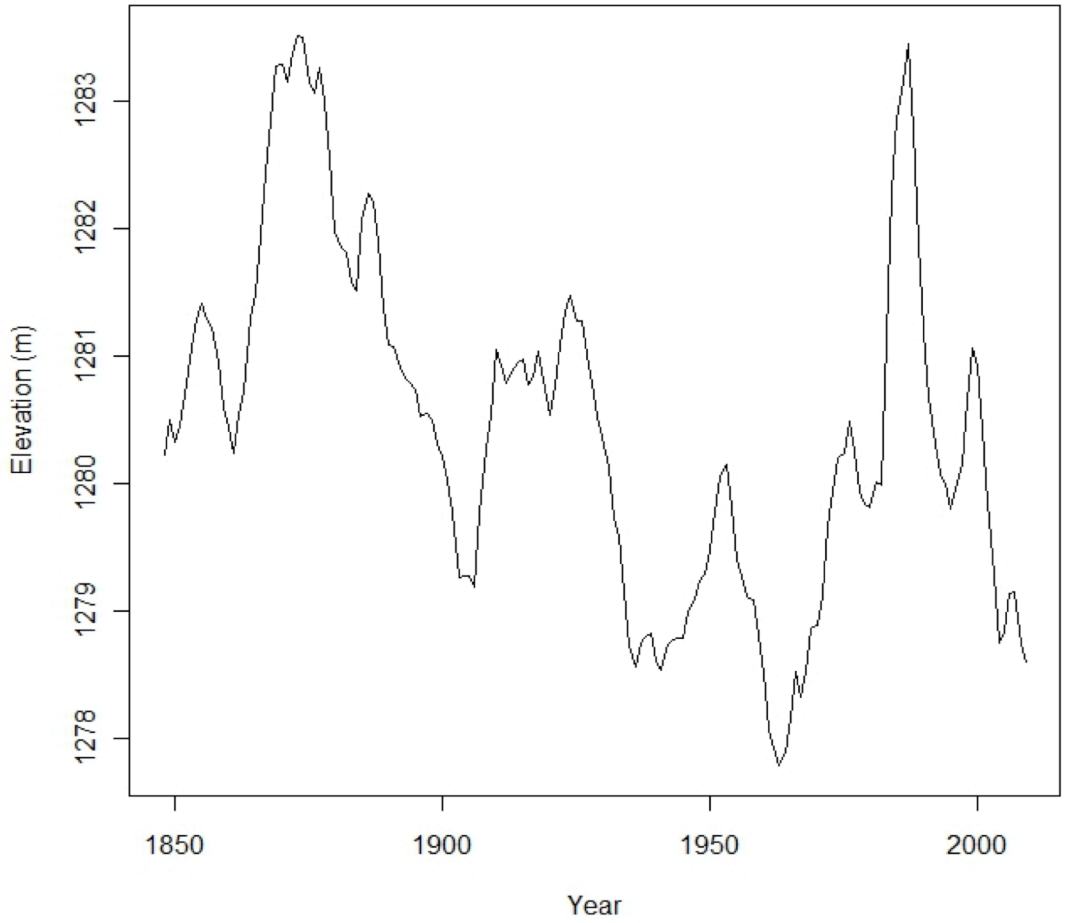

Figure 9. Historical elevations of the Great Salt Lake

Another heuristic model was constructed to evaluate the effect of the short-term variation. The lake elevation for the years 1848 through 2009 is available from the Saltair Boat Harbor monitoring site (USGS, 2001), as shown in Figure 9. The year-to-year variation can be modeled as a second-order autoregressive process AR(2) (Brockwell and Davis, 1991), a model that accounts for year to year temporal correlations in the variation. An AR(2) process was simulated and added to a transgressive or regressive curve based on the simplified model of Section 21. Examples of these simulations are given in Figure 10. As can be seen in the figure, the short-term variation can result in lakes covering the Clive elevation for a short time, receding for a short time, then rising again, often multiple times in a single transgression cycle. A similar simulation was performed for simulated intermediate duration lakes as well. The transgressive and regressive phases of a deep lake are assumed to behave similarly to the intermediate lakes in that they averaged about four total occurrences of "mini-lakes;" i.e., occurrences of a rise above the elevation of Clive followed by a drop below for at least one year.

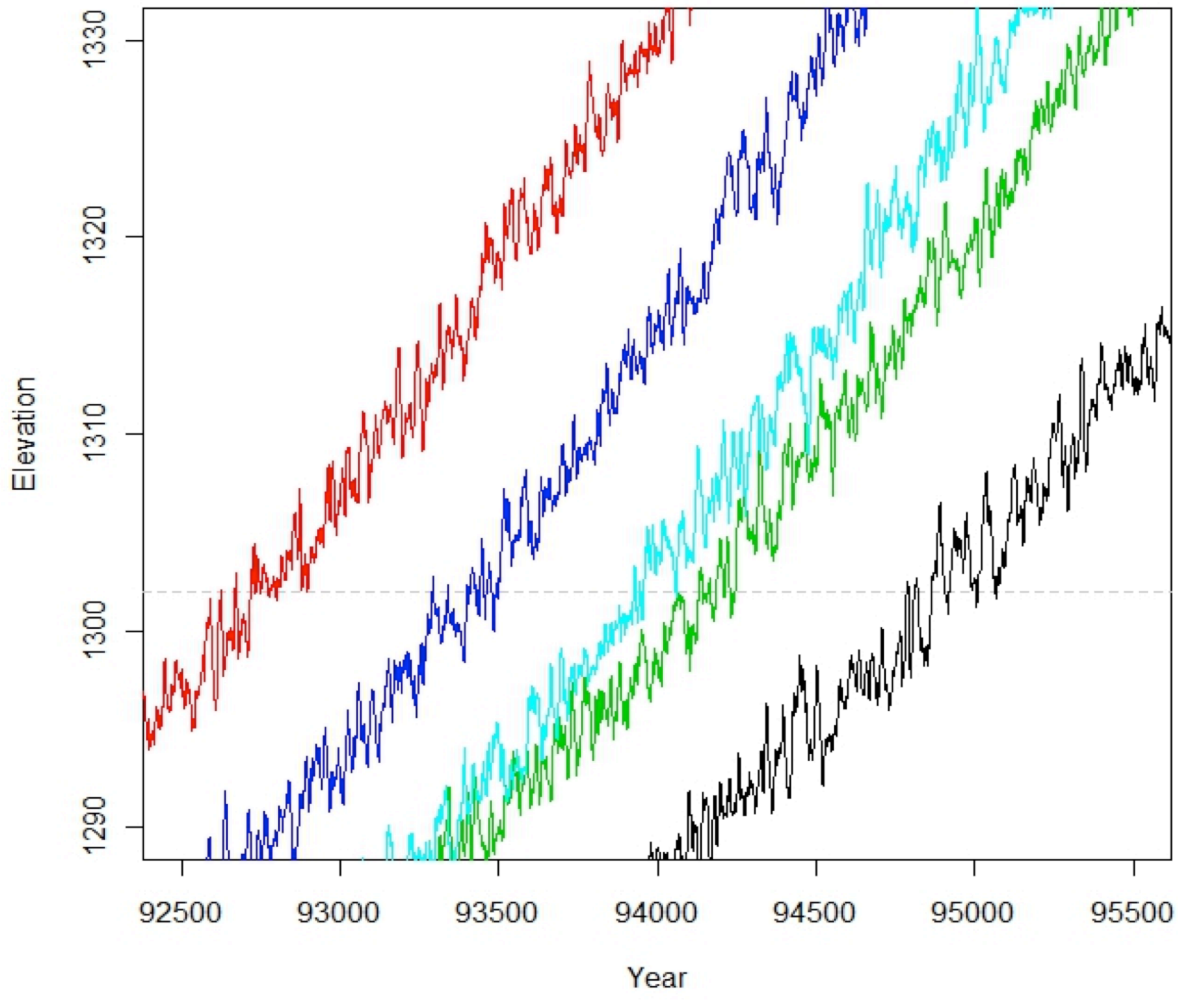

Figure 10. Simulated transgressions of a deep lake including short-term variations in lake elevations

The distribution for sedimentation rates for intermediate lakes was thus based on simulating this multiple mini-lake behavior. First, the number of mini-lakes associated with an intermediate lake was simulated as 1 plus a Poisson random variable with rate 3 (the "plus 1" being necessary to ensure at least one event in order to match the definition of a lake event). The sedimentation for each mini-lake was simulated according to a distribution based on the information for mini-lakes in the Clive pit wall, using the six distinct "mini-lakes" in Table 3 (all layers except the one that corresponds to the deep-water phase of Lake Bonneville), which resulted in a lognormal distribution with geometric mean 0.75 m and geometric standard deviation 1.4. The total sedimentation for all mini-lakes associated with a simulated intermediate lake cycle was then added together to produce a total sedimentation for the intermediate lake. A distribution was then based on all simulated intermediate lake sedimentations, a lognormal distribution with geometric mean 2.82 m and geometric standard deviation 1.71, as presented in Figure 11.

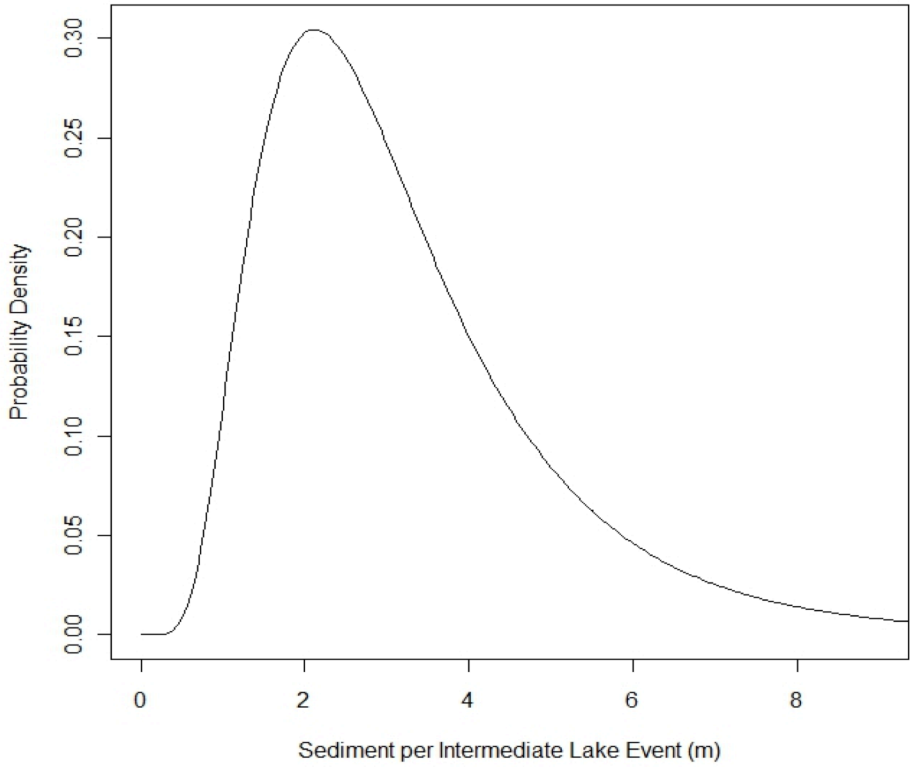

Figure 11. Probability density function for the total sediment thickness associated with an intermediate lake (or the transgressive of regressive phase of a deep lake)

The net effect is that the sedimentation rates are on the order of 15 to 20 m per glacial cycle (100-ky). For the duration of the model (2.1 My), this implies sedimentation of more than 300 m. The Basin and Range system accommodates this rate of sedimentation because it is an extensional system; e.g., sedimentation continues as the basins expand and subside, maintaining similar elevation in each cycle.

6.4 Destruction of the Federal DU Cell

A scenario involving destruction of the Federal DU Cell was modeled. Intermediate lakes are assumed to have sufficient wave energy to destroy the above-ground portions of the DU waste cell. This differentiates a shallow lake from an intermediate lake. The precise elevation needed for this to happen is not considered for the model, but the intermediate lakes that occur in the model are intended to match this definition.

The first lake in the time period assessed is more likely to be an intermediate lake but can be either an intermediate or a deep lake. The destructive energy is equivalent in either case, as the conceptual model treats the transgressive phase of a deep lake as behaving similarly to an intermediate lake.

The mass of material that is within the embankment above the grade of the surrounding land is assumed to be dispersed by wave action. This volume of above grade material in the embankment, including fill material and cap material, is assumed to be mixed with the sediment associated with the intermediate lake, and subsequently spread across the dispersal area. If the user has set up the model to place all DU waste below present-day grade, there is no waste in this material. While our expectation of future events is that the volume of material below grade is simply covered by sediment, the calculations in the Clive DU PA Model v1.2 assume that the DU waste in the below grade layers is also included in the dispersed material as a highly conservative assumption.

A probability distribution for the area across which the embankment material is spread was developed based on an assumption that a destroyed site would be flattened by wave action. The probability distribution for the area was developed so that:

- at a minimum, an area that would be covered if the volume of the above-grade material were spread out to a height of 1 m, and
- an area that would be covered if the volume of the above-grade material were spread out to a height of 10 cm as a geometric mean.

The exact distribution for area depends on the precise volume of the above-grade embankment at the time of destruction, but a lognormal distribution with geometric standard deviation 1.5, and geometric mean defined as above. A typical probability density function is shown in **Error! Reference source not found.**.

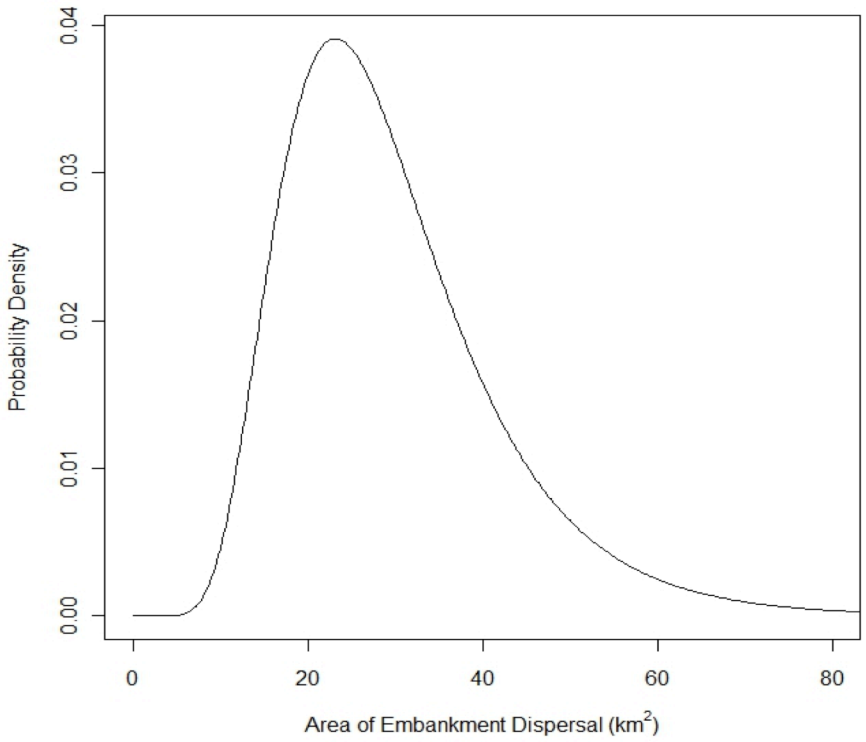

Figure 12. Probability density function for the area over which the waste embankment is dispersed upon destruction

6.5 Reported Results

As a qualitative assessment, the deep time model does not calculate dose to human receptors, but rather characterizes the fate of the bulk of the waste. After the destruction of the waste embankment, the bulk of the waste will be mixed with lake sediments and a portion of the inventory dissolved in lake water.

Upon destruction of the waste embankment, the PA model switches modes from detailed modeling of waste transport through air dispersion, biotic uptake, groundwater flow, and other processes to a much simpler model. These processes are expected to have minor effects on transport once the waste is mixed into a sedimentary layer. The only processes that are modeled after destruction are lake recurrence, radioactive decay and ingrowth, mixing of waste with sediment, and dissolution of waste in lake water.

6.5.1 Concentration in Sediment

A scenario considering occurrence of an intermediate lake, the resulting destruction of the Energy*Solutions* waste embankment, and dispersal of the waste is modeled. The activity per unit volume of sediment following the dispersal of the waste is estimated using Equation 13 below.

The model calculates radioactivity by volume in the sediment layers, after the embankment has been destroyed. The current implementation always mixes sediment with the full amount of

waste, and does not consider a mixing depth; i.e., the waste is always fully mixed and not covered by sediment. Thus, radioactivity concentration in sediment is initially calculated under the assumption that all of the waste in the waste embankment is mixed evenly with the sediment that forms as a result of the lake destroying the embankment.

Concentration in sediment is initially calculated under the assumption that all of the waste that was above grade in the waste embankment is mixed evenly with the sediment that forms with the lake that destroys the site[7].

$$C_{\text{sediment}} = \frac{R_{\text{embankment}}}{V_{\text{material above grade}} + V_{\text{sediment}}}. \quad (13)$$

where

$R_{\text{embankment}}$	is all remaining radioactivity in the embankment,
$V_{\text{material above grade}}$	is the volume of material in the above grade portion of the embankment, and
V_{sediment}	is calculated as the depth of sediment due to lake processes multiplied by the area over which the waste is dispersed.

This calculation assumes that there is no loss of waste from the initial dispersal region. While this calculation is counter to the modeling of dissolution into the water column of the lake, a simplifying assumption is that all waste that dissolves into the lake precipitates back into the sediment upon recession of the lake.

The concentrations in sediment are modeled as remaining constant, except for decay and ingrowth, until a new lake occurs. When a new lake occurs, the sedimentation associated with that lake is likely to mix with some portion of the top layer of existing sediment and leave the lower layers of the sediment buried beneath. However, for simplicity, a conservative approach is to mix all sediment that contains waste, effectively keeping some portion of the waste near-surface. The concentration is again the total radioactivity divided by the volume containing waste, but the volume that contains waste now has the additional volume of sediment associated with the current lake.

6.5.2 Radioactivity in Lake Water

When lake water is present, radionuclides will partition between the water phase and the solid phase depending on element-specific solubility and sorption properties. Radionuclides remaining in the pore water will then diffuse into the lake. The waste is likely to mix over a wide area of the lake, and many forms of the waste are likely to bind with carbonate ions in the water, ultimately precipitating into carbonate sediments. As a conservative assumption, upon recession of the lake, all waste is assumed to precipitate back into the *local* sediments, meaning that all radionuclides in the sediments modeled in Section 37 are returned to the sediments when the lake regresses.

When a lake returns, the sediments are assumed to be fully saturated, and radionuclides are partitioned from the sediment to the pore water within the sediment using the same partitioning

[7] See footnote 4.

coefficients (K_d) used for other sedimentary soils in the model. An important difference between the assumptions for this model and the model for transport from the embankment in the 10-ky model is that the lake water is assigned a different solubility for uranium for the deep time assessment. While solubilities for all other radionuclides remain the same, the solubility for uranium is reduced to that of U_3O_8 which is significantly lower than other forms of uranium originally present in the waste. This change in solubility for uranium is adopted because it is expected that by the time the first lake returns, all soluble uranium forms (UO_2 and UO_3) will have been leached from the embankment into the shallow aquifer.

As radionuclides associated with the sediments dissolve into the pore water, they diffuse into the lake water using a constant flux model based on Fick's first law, with the following assumptions:

- There is an interface boundary layer of 0.1 m above the sediment, above which the water has a radionuclide concentration of 0. In fact, there will be some buildup of concentration as a radionuclide migrates into the water, but it will diffuse into the lake. It is conservative to assume a zero concentration, which results in the highest possible flux.
- The concentration in sediment remains constant over the deep time period. The sediment concentration should in fact diminish over time if enough mass is migrated into the water, but for simplicity, the sediment concentrations are kept constant across time steps.

Fick's law for this case estimates the mass diffusing from a given volume of sediment into the lake with time. The mass (or activity) per area per time is the flux. Fick's law states that this flux is given by the difference in mass concentration over a distance (the concentration gradient) multiplied by a free-water diffusion coefficient, across a diffusive area. The calculation assumes that there is a stagnant interface boundary layer of water between the sediment and the open water that is 0.1 m thick. The assumption is also made that the mass concentration is zero in the open water. The difference in concentration across the stagnant layer is then the concentration in the sediment C_v minus the concentration in the open water or $C_v - 0$ g/mL. Fick's law applied to diffusion is used to define the mass (or activity) flux J:

$$J = \frac{R}{\Delta t\, A} = D_m \frac{C_v}{b_{bdy}}$$

where

R is the mass (M) activity (T^{-1}),
ΔT is the length of the time period (T),
A is the area of the sediment that contains the waste (L^2),
D_m is the diffusion coefficient for the radionuclide in water (L^2/T), and
b_{bdy} is the thickness of the boundary layer.

Multiplying both sides of the equation by $\Delta T \cdot A$ gives

$$R = \Delta T \cdot D_m \cdot \frac{C_V}{0.1\ \text{m}} \cdot A, \qquad (14)$$

Concentration in lake water is calculated based on the conservative assumption that the radioactive material does not dilute in a large basin of the lake but rather remains in the water column immediately above the dispersed area. The activity concentration in the lake water is then calculated by dividing the total activity, R, by the volume of lake water. The volume of lake water is the product of the lake depth and the dispersal area:

$$C_v = \frac{R}{D \cdot A} \tag{15}$$

where

- C_v is concentration (M/L^3 or T^{-1}/L^3),
- R is the mass (M) or radioactivity (T^{-1}),
- A is the area of the sediment that contains waste (the dispersed area, as L^2), and
- D is the depth of the lake (L).

The above equations are implemented in the Clive DU PA Model to provide qualitative assessments of deep time concentrations in lake water and lake sediment following the return of a lake in the Bonneville Basin large enough to demolish the Federal DU Cell.

There is an insufficient record of lake elevations to construct a data-based distribution for lake depth. Thus, the distributions for lake depth are chosen based on the conceptual model. Depths for intermediate lakes have a Beta distribution with mean of 30 m, standard deviation 18 m, minimum of 0 m, and maximum of 100 m. Depths for deep lakes have a Beta distribution with mean 150 m, standard deviation 20 m, minimum of 100 m, and maximum of 200 m.

For intermediate lakes, the time step is the duration of the intermediate lake. For deep lakes, the lake may exist for several time steps in the GoldSim model, in which case the time step is the portion of the time step for which the lake is present. When deep lakes cross multiple time steps, the concentration in sediment is allowed to change between time steps (only due to decay and ingrowth), and the activity in the lake water is accumulated over those time steps.

7.0 References

Adams, K.D., 2003, Age and paleoclimatic significance of late Holocene lakes in the Carson Sink, NV, USA, *Quaternary Research*, Vol. 60, pp. 294–306, 2003.

Archer, D. and A. Ganopolski, 2005. A movable trigger: fossil fuel CO_2 and the onset of the next glaciation. *Geochemistry, Geophysics, Geosystems*, 6(5), doi:10.1029/2004GC000891.

Asmerom, Y., Polyak, V. J., and S. J. Burns, 2010. Variable winter moisture in the southwestern United States linked to rapid glacial climate shifts. *Nature Geoscience*, 3, 114-117.

Balch D.P., A.S. Cohen, D.W. Schnurrenberger, B.J. Haskell, B.L.V. Garces, J.W. Beck, H. Cheng, and R.L. Edwards, 2005. Ecosystem and paleohydrological response to Quaternary climate change in the Bonneville basin, Utah, *Palaeogeography, Palaeoclimatology, Palaeoecology*, Vol. 221, pp. 99–121.

Berger, A., 1988. Milankovitch theory and climate. *Reviews of Geophysics*, 26(4): 624-657.

Berger, A. and M. F. Loutre, 2002. An exceptionally long interglacial ahead? *Science*, 297: 1287-1288.

Benson, L.V., S.P. Lund, J.P. Smoot, D.E. Rhode, R.J. Spencer, K.L. Verosub, L.A. Louderback, C.A. Johnson, R.O Rye, R.M. Negrini, 2011, *The Rise and Fall of Lake Bonneville Between 45 and 10.5 ka,* Quaternary International, Vol. 235, p. 57-69.

Briggs, R.W., S.G. Wesnousky, and K.D. Adams, 2005, Late Pleistocene and late Holocene lake highstands in the Pyramid Lake subbasin of Lake Lahontan, Nevada, USA, *Quaternary Research,* Vol. 64, pp. 257–263, 2005.

Brimhall W. H. and L. B. Merritt, 1981. The geology of Utah Lake – implications for resource management. *Great Basin Naturalist Memoirs*, 5: 24-42.

Brockwell, P.J. and R.A. Davis, 1991. *Time Series: Theory and Methods*. Springer-Verlag, New York, NY.

Clark, P. U., Dyke, A. S., Shakun, J. D., Carlson, A. E., Clark, J., Wohlfarth, B., Mitrovica, J. X., Hostetler, S. W., and A. M. McCabe, 2009. The Last Glacial Maximum. *Science*, 325: 710-714.

Cochelin, Anne-Sophie B., L.A. Mysak, Z. Wang, 2006, Simulation of long-term future climate changes with the green McGill paleoclimate model: The next glacial inception. *Climate Change,* 79, 381-401.

Currey, D.R., G. Atwood, and D.R. Mabey, *Map 73 Major Levels of Great Salt Lake and Lake Bonneville*, Utah Geological and Mineral Survey, Salt Lake City, UT, May 1984

Davis, O.K., 1998. Palynological evidence for vegetation cycles in a 1.5 million year pollen record from the Great Salt Lake, Utah, *U.S.A.*, *Palaeogeography, Palaeoclimatology, Palaeoecology*, Vol. 138, pp. 175–185.

Driscoll, N. W. and G. H. Haug, 1998. A short circuit in thermohaline circulation: a cause for Northern Hemisphere glaciation. *Science*, 282: 436-438.

Einselle, G. and M. Hinderer, 1997. Terrestrial sediment yield and the lifetimes of reservoirs, lakes, and larger basins. *Geologische Rundschau*, 86: 288-310.

EPICA community members, 2004. Eight glacial cycles from an Antarctic ice core. *Nature*, 429: 623-628.

Fritz, S.C., 1996, Paleolimnological records of climatic change in North America, *Limnol. Oceanogr.* 45, 882-889.

GTG (GoldSim Technology Group), 2011. *GoldSim: Monte Carlo Simulation Software for Decision and Risk Analysis*, http://www.goldsim.com

Hart, W. S., Quade, J., Madsen, D. B., Kaufmann, D. S., and C. G. Oviatt, 2004. The $^{87}Sr/^{86}Sr$ Ratios of Lacustrine Carbonates and Lake-level History of the Bonneville Paleolake System. *GSA Bulletin*, 116: 1107-1119.

Haug, G. H. and R. Tiedemann, 1998. Effect of the Formation of the Isthmus of Panama on Atlantic Ocean Thermohaline Circulation. *Nature*, 393: 673-676.

Hays, J. D., Imbire, J., and N. J. Shackleton, 1976. Variations in the Earth's Orbit: Pacemaker of the Ice Ages. *Science*, 194: 1121-1132.

Jansen, E. J. Overpeck, K.R. Briffa, J.-C. Duplessy, F. Joosv, V. Masson-Delmotte, D. Olago, B. Otto-Bliesner, W.R. Peltier, S. Rahmstorf, R. Ramesh, D.. Raynaud, D. Rind, O. Solomina, R. Villalba, and D. Zang, 2007, Palaeoclimate. In: *Climate Change 2007: The Physical Science Basis. Contribution of Working Group I to the fourth Assessment Report of the Intergovernmental Panel on Climate Change* [Solomon, s. D. Qin, M. Manning, Z. Chen, M. Marquis, K.B. Averyt, M. Tigor and H.L Miller (eds.)] Cambridge University Press, Cambridge, United Kingdom and New York, NY, USA.

Jewell, P.W. 2010, River incision, circulation, and wind regime of Pleistocene Lake Bonneville, USA, *Palaeogeography, Palaeoclimatology, Palaeoecology,* 293, 41-50.

Jouzel, J., Masson-Delmotte, V., Cattani, O., Dreyfus, G., *et al.*, 2007. Orbital and millennial Antarctic climate variability over the past 800,000 years. *Science*, 317: 793-796.

Kukla, G. J., R. K. Matthews, J. M. Mitchell Jr., *Quat. Res.* **2**, 261 (1972)

Lisiecki, L. E. and M. E. Raymo, 2005. A Pliocene-Pleistocene stack of 57 globally distributed benthic $\delta^{18}O$ records. *Paleoceanography*, 20, PA1003, doi:10.1029/2004PA001071.

Link, P. K., Kaufmann, D. S., and Thackray, G. D., 1999. Field guide to Pleistocene lakes Thatcher and Bonneville and the Bonneville flood, southeastern Idaho, *In*: Hughes S. S. and G. D Thackray (eds.), *Guidebook to the Geology of Eastern Idaho*, Idaho Museum of Natural History, p. 251-266.

Lyle, M., L. Heusser, C. Rovelo, M. Yamamoto, J. Barron, N.S. Diffenbaugh, T. Herbert, D. Andreasen, 2012, Out of the Tropics: The Pacific, Great Basin Lakes, and Late Pleistocene Water Cycle in the Western United States, *Science*, Vol. 337, p. 1629–1633.

Machette, M.N., S.F. Personius, and A.R. Nelson, 1992. Paleoseismology of the Wasatch fault zone: A summary of recent investigations, interpretations, and conclusions, in Gori, P.L., and

W.W. Hays, eds., *Assessment of regional earthquake hazards and risk along the Wasatch Front, Utah,* U.S. Geological Survey Professional Paper 1500-A-J, pp. A1–A71, 1992.

Madsen, D.B., 2000. *Late Quaternary Paleoecology in the Bonneville Basin*, Utah Geological Survey Bulletin 130, 2000.

Masson-Delmotte, V., Stenni, B., Pol, K., Braconnot, P., *et al.*, 2010. EPICA Dome C record of glacial and interglacial intensities. *Quaternary Science Reviews*, 29: 113-128.

Masson-Delmotte, V., M. Schulz, A. Abe-Ouchi, J. Beer, A. Ganopolski, J.F. Gonzalez Rouco, E. Jansen, K. Lambeck, J. Luterbacher, T. Naish, T. Osborn, B. Otto-Bliesner, T. Quinn, R.. Ramesh, M. Rojas, X. Shao, and A. Timmermann, 2013, Information from Paleoclimate Arechive. In: *Climate Change 2013: The Physical Science Basis. Contribution of Working group I to the Fifth Assessment Report of the Intergovernmental Panel on Climate Change,* Stocker, T.F., D. Qin, G.-K. Plattner, M. Tignor, S.K. Allen, J. Boschung, A. Nauels, Y. Xia, V. Bex and P.M. Midgley (eds.)]. Cambridge University Press, Cambridge, United Kingdom and New York, NY, USA.

Matsurba, Y. and A. D. Howard, 2009. A spatially explicit model of runoff, evaporation, and lake extent: application to modern and late Pleistocene lakes in the Great Basin region, western United States. *Water Resources Research*, 45, W06425, doi:10.1029/2007WR005953.

Miller, D.M., C.G. Oviatt, and J.P. Mcgeehin, 2013. Stratigraphy and chronology of Provo shoreline deposits and lake-level implications, Late Pleistocene Lake Bonneville, eastern Great Basin, U.S.A., *Boreas*, Vol. 42, pp. 342–361, 2013.

Nash, W.P., 1990*, Black Rock Desert, Utah*, in C.A Woods and J. Kienle, eds. Volcanoes of North America, Cambridge University Press, Cambridge p. 271-273.

Oviatt, C. G. and W. P. Nash, 1989. Late Pleistocene basaltic ash and volcanic eruptions in the Bonneville basin, Utah. *Geological Society of America Bulletin*, 101: 292-303.

Oviatt, C. G., McCoy, W. D., and Nash, W. P., 1994a. Sequence stratigraphy of lacustrine deposits: a Quaternary example from the Bonneville basin, Utah. *Geological Society of America Bulletin,* 106: 133-144.

Oviatt, C.G., G.D. Habiger and J.E. Hay, 1994b. *Variation in the Composition of Lake Bonneville Marl: A Potential Key to Lake-Level Fluctuations and Paleoclimate,* Journal of Paleolimnology, Vol 11, p. 19-30.

Oviatt, C. G., 1997. Lake Bonneville fluctuations and global climate change. *Geology*, 25(2): 155-158.

Oviatt, C. G., Thompson, R. S., Kauffman, D. S., Bright, J., and R. M. Forester, 1999. Reinterpretation of the Burmester core, Bonneville Basin, Utah. *Quaternary Research*, 52: 180-184.

Oviatt, C.G.,2002, *Comparing the Shoreline and Offshore Sedimentary Records of Lake Bonneville*. Abstracts with Programs - Geological Society of America 34(6): 292.

Oviatt, C. G., D. M. Miller, J. P. McGeehin, C. Zachary, and S. Mahan, 2005. The Younger Dryas phase of Great Salt Lake, Utah, USA, *Palaeogeography, Palaeoclimatology, Palaeoecology*, 219: 263-284.

Oviatt, C.G., and B. P. Nash, 2014, *The Pony Express Basaltic Ash: A Stratigraphic Marker in Lake Bonneville Sediments, Utah,* Miscellaneous Publication 14-1, Utah Geological Survey 10 p.

Paillard, D., 2001. Glacial cycles: toward a new paradigm. *Reviews of Geophysics*, 39(3): 325-346.

Paillard, D., 2006. What drives the Ice Age cycle? *Science*, 313: 455-456.

Ruddiman, W.F., 2006. Orbital Changes and Climate, *Quaternary Science Reviews*, Vol. 25, pp. 3092–3112.

Schnurrenber, D. J. Russell, and K Kelts, 2003, Classification of lacustrine sediments based on sedimentary components, *Journal of Paleolimnology* 29, p. 141-154.

Schofield, I., P. Jewell, M. Chan, D. Currey, and M. Gregory, 2004, Shoreline development, longshore transport, and surface water dynamics, Pleistocene Lake Bonneville, Utah, *Earth Surf. Process. Landforms,* 29, 167-1690.

Tzedakis, P.C., E.W. Wolff, L.C. Skinner, V. Brovkin, d.A. Hodell, J.F. McManus, and D. Raynaud, 2012a, Can we predict the duration of an interglacial? *Climate Past 8, 1473-1485.*

Tzedakis, P.C., J.E.T. Channel, D.A. Hodell, H.F. Kleiven, and L.C. Skinner, 2012b, Determining the natural length of the current interglacial, *Nature Geoscience,* 5, 138-141.

United States Geological Survey (USGS), 2001. National Water Information System data (Water Data for the Nation), accessed December, 2010 URL: http://waterdata.usgs.gov

Appendix A

A.1 Clive Pit Wall Interpretation (C. G. Oviatt, unpublished data)

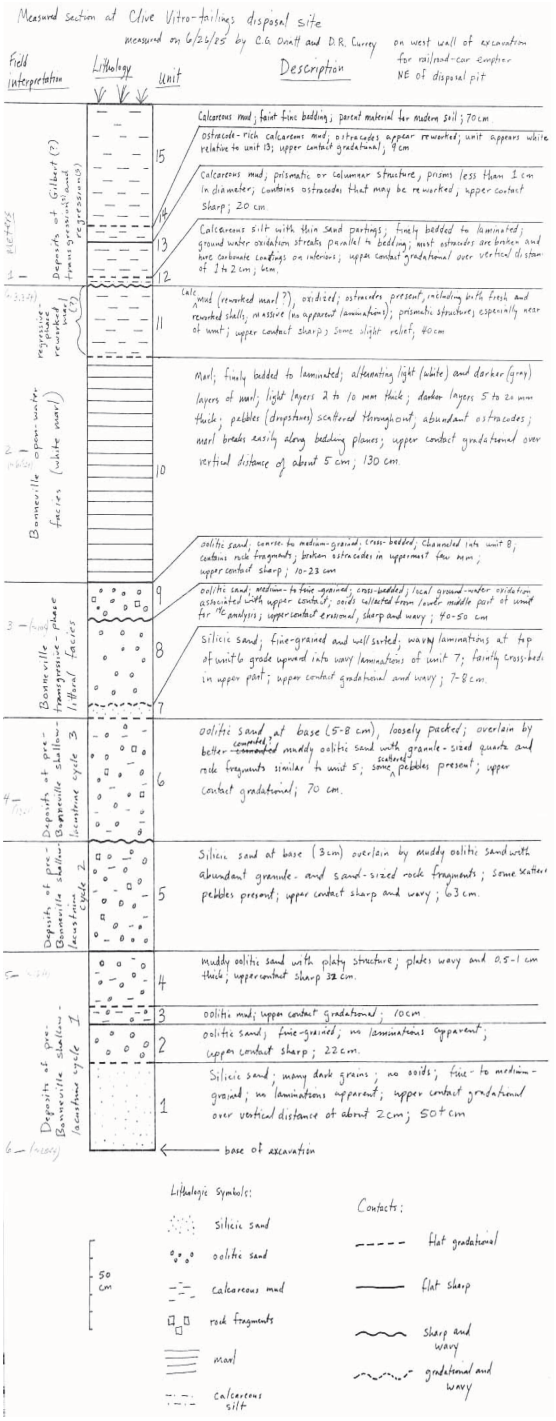

Appendix B

B.1 Knolls Core Interpretation (C. G. Oviatt, unpublished data)

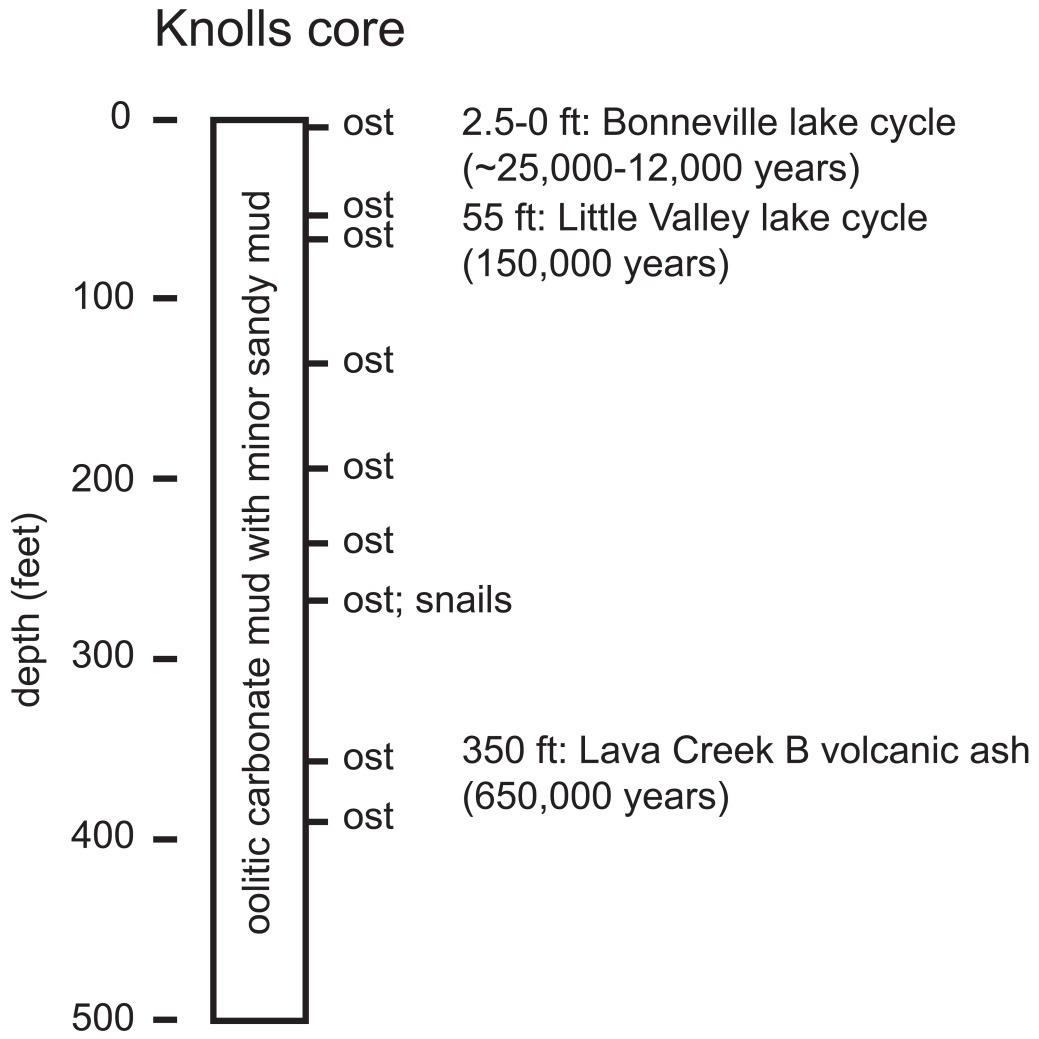

ost = ostracodes (fresh water of a lake or marsh)
snails indicate shallow fresh water